Sox genes represent a family related by the *Sry*-type high-mobility group (HMG) box, and function as transcription factors in various developmental processes through binding to a conserved core DNA sequence [16]. Twenty *Sox* genes have been identified in mouse and human, and are classified by their HMG box sequences into subgroups A–H [17, 18]. The expression pattern of each gene tends to be conserved in mouse and chicken. Among them, *Sox9* (group E) is known to act as a sex-determining gene. Mutations of human *SOX9* cause campomelic dysplasia, a severe skeletal malformation syndrome associated in most cases with XY sex reversal [19, 20], and ectopic expression of *Sox9* in XX mouse fetal gonads induces testis formation [21].

AMH plays an important role in inducing the regression of the Müllerian ducts in males, which normally give rise to the uterus, oviducts, upper vagina and fallopian tubes in females [22]. Analysis of mouse and human *Amh* gene regulation has uncovered several factors important for modulating *Amh* expression. For example, SF1 up-regulates *Amh* expression by cooperative interaction with WT1 [23], GATA-4 [24], SOX9 [25] and SOX8 [26]. Mice mutant for the SOX-binding site or the SF1-binding site in the *Amh* promoter revealed that SOX proteins are essential for *Amh* expression, while SF1 enhances the final expression level [27]. Oréal et al. [28] were the first to describe the chicken *Amh* promoter and showed that it has little overall homology with the mouse *Amh* promoter, but contains two putative SOX-binding sites and one SF1-binding site, suggesting that the mouse and chicken *Amh* promoters are similarly regulated. However, chicken *Sox9* is expressed too late to be a *cAmh* regulator [28, 29], but another SOX protein might substitute for SOX9 and, together with SF1, regulate *cAmh* expression.

Previously, we hypothesized that SOX8 might be a candidate transcription factor for regulating the chicken *Amh* gene [26, 30]. Mouse *Sox8* is expressed male specifically during gonad development. Its expression starts prior to the onset of *Amh* gene expression, and encodes a protein product that can up-regulate mouse *Amh* together with SF1 in vitro [26]. Group E Sox genes, consisting of Sox8, Sox9 and Sox10, show moderate levels of amino acid similarity and have similar genomic organization, suggesting that group E *Sox* genes may originate from one ancestral gene [31]. Although expression patterns of *Sox9* and *Sox10* overlap to a limited extent [32, 33], expression of *Sox8* overlaps substantially with expression of *Sox9* [31, 32] and to a lesser extent, *Sox10* [33, 31]. This fact suggests that there is some functional redundancy between SOX8 and SOX9, similar to that published for SOX1, SOX2 and SOX3 in lens formation [34], L-SOX5 and SOX6 in cartilage formation [35] and SOX7, SOX17 and SOX18 in vasculogenesis [36–38].

In this study, we analyzed the expression patterns of chicken *Sox8* in developing gonads during the sex-determining window. If *cSox8* contributes to *cAmh* gene expression, one would expect to find *cSox8* predominantly expressed in the embryonic testis and prior to the onset of *cAmh*. We found this not to be the case, suggesting that SOX8 is not responsible for sex-specific expression of *cAmh* in chicken. We also tested the expression patterns of several other *cSox* genes which are expressed in embryonic testis, and similarly found that they were not expressed male specifically.

Materials and methods

Chicken embryos. Fertilized chicken eggs were obtained from local suppliers (Ingham, Brisbane, Australia and Saitama Experimental Animal Supply, Saitama, Japan) and maintained at 18 °C until use. Eggs were transferred to an incubator at 37.5 °C and allowed to develop for 5, 6 or 7 days. Staging was confirmed at dissection according to Hamburger and Hamilton [39]. The entire urogenital ridge of each embryo was explanted for whole-mount *in situ* hybridization. Sexing was performed by PCR as described elsewhere [40] using genomic DNA purified from a hind limb of each embryo.

Amplification of HMG box sequences. Total RNA was isolated from left and right gonads of day 6 male embryos by standard methods [41]. RNA (0.5 μg) was then treated with DNaseI and first-strand cDNA was synthesized using M-MLV reverse transcriptase (Invitrogen) according to the manufacturer's protocol. For amplification of the HMG box, the PCR reaction was carried out in a solution containing 1 x NH_4 buffer (Bioline), 100 M $MgCl_2$, 100 μM dNTPs, 0.4 μM primers and 0.5 unit Biotaq DNA polymerase (Bioline) with 4.5 min denaturation at 95 °C followed by 40 cycles of amplification at 95 °C for 30 s and 57 °C for 30 s. The PCR product was cloned into pGEM-T Easy (Promega). Sequencing was performed using the BigDye Terminator v3.1 Cycle Sequencing Kit (Applied Biosystems) and M13 reverse primer, and electrophoresis was carried out by the Australian Genome Research Facility, Brisbane, Australia. Primer sequences used were as follows; G7A1: 5'-AGC G(A/G)C CCA TGA ACG C(A/C/G/T)T T-3' and G7B1: 5'-CGC (C/T)GG TA(C/T) TT(A/G) TA(A/G) TC(A/C) GGG T-3'. The PCR reaction was also carried out using genomic DNA as a template.

RT-PCR of *Sox* genes, *Amh* and *Actin*. The left and right gonads of staged, sexed embryos were pooled (ten and five embryos of each sex for day 6 and day 7, respectively) to isolate total RNA using the RNeasy Mini kit (Qiagen) with the optional on-column DNase digestion with the RNase-free DNase set. The first-strand cDNA was synthesized from 1 μg of total RNA using Power-

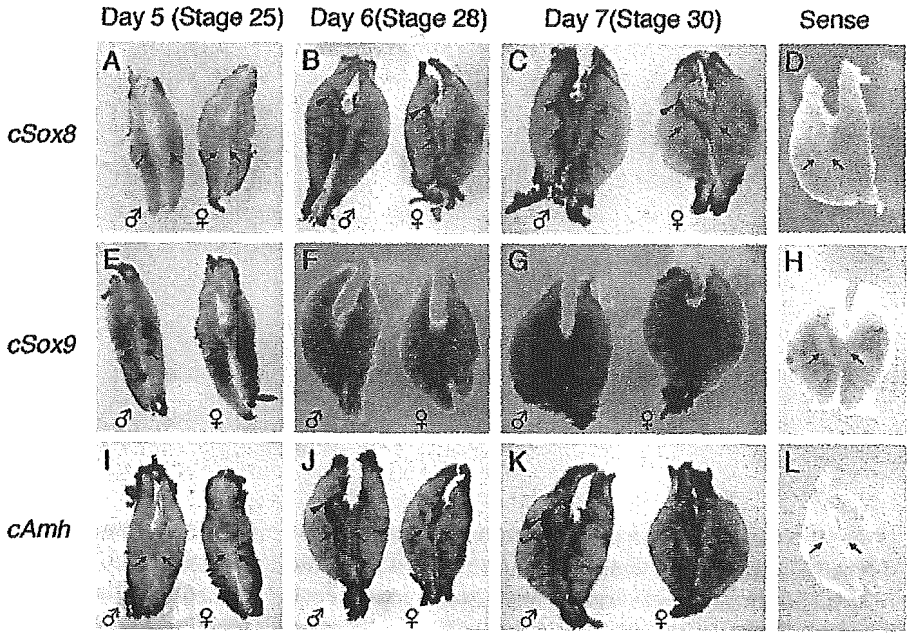

Figure 1. Whole-mount *in situ* hybridization of *cSox8*, *cSox9* and *cAmh* in the chicken embryonic gonad/mesonephros. In each panel, male (♂) and female (♀) gonad/mesonephros are left and right, respectively. Probes used are shown at the left of each panel. The samples in A–C, E–G and I–K were hybridized with antisense probe. In D and L a day 6 sample hybridized with sense probe. In H a day 7 sample was hybridized with sense probe. Developmental stages (days and Hamburger-Hamilton stage) of gonad/mesonephros are labeled above. Arrow shows the position of gonad. Arrowheads point to regions of positive staining.

Script reverse transcriptase (Clontech) and oligodT. PCR amplification was carried out using the QuantiTect SYBR Green PCR kit (Qiagen) with uracil-N-glycosylase and the 7900HT Sequence Detection System (Applied Biosystems). Samples were incubated at 50 °C for 2 min, then 95 °C for 15 min, followed by 40 cycles of amplification at 94 °C for 30 s, 54.2 °C for 1 min and 72 °C for 1 min. For the amplification of *cSox8* and *cSox9*, 85.4 °C for 15sec was added after each 72 °C step of each amplification cycle. Primer sequences used were as follows; cSox3-1: 5'-GCACCAGCACTACCAGAG-3' and cSox3-2: 5'-CGA ATG CGG ACA CGA ACC) for *cSox3* [29], cSox4F: 5'-TCG GGG GAT TGG CTG GAG TC-3' and cSox4R: 5'- CTC AGC CGA TCC TCG TTT CC-3' for *cSox4*, cSox8RTF : 5'-CTA CAA GGC TGA CAG CGG GC-3' and cSox8RTR: 5'-AGG CCG GGC TCT TGT GAG TC-3' for *cSox8*, cSox9F: 5'-CCC CAA CGC CAT CTT CAA-3' and cSox9R: 5'-CTG CTG ATG CCG TAG GTA-3' for *cSox9*, cSox11F2: 5'-AAG CAG GAG GCG GAC GAC GA-3' and cSox11R2: 5'-CGC CCC GCA CCT CCT CGT AG-3' for *cSox11*, cAmh-1: 5'-GTG GAT GTG GCT CCC TAC CC-3' and cAmh-2: 5'-GCA GCA CCG AGG GCT CCT CC-3' for *cAmh* [29] and Actin-1: 5'-TGG ATG ATG ATA TTG CTG C-3' and Actin-2: 5'-ATC TTC TCC ATA TCA TCC C-3' [29] for *Actin*. To calculate the relative amount of gene expression levels, the $\Delta\Delta C_T$ method was used. Three independent pooled samples were analyzed. Maximum average values were set as 100%.

For the RT-PCR amplification of *cSox12* and *cSox14*, the same cDNA for the real-time RT-PCR was used. The PCR reaction was carried out in the same solution as HMG box amplification with 4.5 min denaturation at 95 °C followed by 40 cycles of amplification at 95 °C for 30 s and 50 °C for 30 s. Primer sequences used were as follows; cSox12F: 5'-AGA TCT CCA AGC GCC TGG GTC G-3' and cSox12R: 5'-GGT AGT CGG CCA TGT GCT TG-3' for *cSox12*, cSox14F: 5'-GAG GTT CCT CAC ACC TTG GC-3' and cSox14R: 5'-ACA CGG AGG AAT CCC AGT CC-3' for *cSox14*.

Probes. The previously reported *cAmh* probe [9] was obtained by RT-PCR amplification of an 821-bp fragment, using primers cAMHRTF (5'-ACG GTG CGC GCC CAC TGG CAG G-3') and cAMHRTR (5'-ACG TCG TGA CCT GCA AGC CCT C-3') and RNA prepared from 5.5-day-old whole embryo. The *cSox8* probe was cloned by PCR using primers chSox8C2F (5'-CTG CAG AGC TCC AAC TAC TAC A-3') and chSox8C2R (5'-GAG CTC TGT CCT TTT GGA GAG T-3') and chicken genomic DNA as the template. The fragment corresponds to nucleotides 1228–1589 of the *cSox8* mRNA sequence (accession No. AF228664). PCR products of *cAmh* and *cSox8* were cloned into the pGEM-T Easy vector. The *cSox9* probe was reported previously by Kent et al. [11]. The *cSox11* fragment was cloned by SacI digestion of *cSox11* cDNA and subsequent insertion into pBluescriptII KS vector. The fragment corresponds to nucleotides 667–967 of the *cSox11* mRNA sequence (accession No. AB012237). The *cSox4* probe was obtained by KspI digestion of *cSox4* cDNA and subsequent insertion into pBluescriptII KS vector. The fragment corresponds to nucleotides 576–965 of the chicken *Sox4* mRNA sequence (accession No. AY493693).

***In situ* hybridization.** Sense and antisense digoxygenin-labeled RNA probes were generated by *in vitro* transcrip-

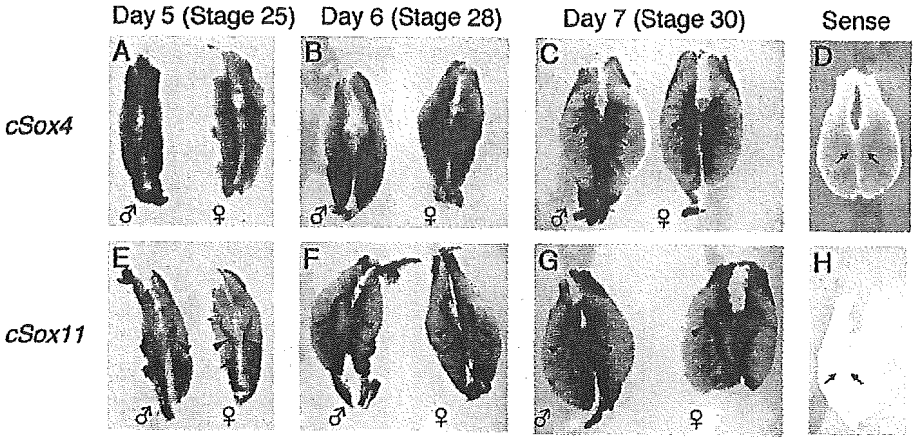

Figure 2. Whole-mount *in situ* hybridization of *cSox4* and *cSox11* in the chicken embryonic gonad/mesonephros. In each panel, male (♂) and female (♀) gonad/mesonephros are left and right, respectively. Probes used are shown at the left of each panel. A–C and E–G were hybridized with antisense probe. D and H show day 6 samples hybridized with sense probe. Developmental stages (days and Hamburger-Hamilton stage) of gonad/mesonephros are labeled above. Arrow shows the position of gonad. Arrowheads point to regions of staining.

tion. Whole mount *in situ* hybridization was performed as described using the maleic acid buffer (MABT) method [42]. Experiments were carried out at least twice for each probe, with similar results.

Results and discussion

To compare the temporospatial expression of *cSox8* and *cAmh* in embryonic gonads, we employed whole-mount *in situ* hybridization analysis using female and male gonad/mesonephros complexes isolated from day 5, 6 and 7 chicken embryos (Hamburger and Hamilton stages 25, 28 and 30, respectively [39]). These stages cover the temporal window at which sexual dimorphism in the gonad first becomes apparent [43]. In addition to providing spatial information relating to gene expression, whole-mount *in situ* hybridization is commonly used as a semiquantitative guide to gene expression levels between different tissues hybridized with the same probe and incubated under the same conditions, as in the experiments described below.

As expected, *cAmh* was expressed at higher levels in male than in female gonads at day 6 and 7 (fig. 1J, K). Expression levels in the right male gonads were higher than in the left, possibly reflecting the asymmetric development of avian genital ridges [43]. We did not observe expression of *cAmh* at day 5 (fig. 1I), even though Oréal et al. [28] reported that *cAmh* is expressed weakly and at similar levels in male and female gonads at day 5 by section *in situ* hybridization. This may reflect lower sensitivity of our whole mount *in situ* hybridization method.

Previous workers have reported that male-specific high-level expression of *cSox9* is preceded by expression of *cAmh* in the chick [28, 29]. We analyzed the temporal expression of *cSox9* in chicken embryos. No signal was observed in male or female gonads at day 5 or day 6 (fig. 1E, F). High levels of *cSox9* expression were observed in day 7 male gonads, while no signal was observed in the day 7 female (fig. 1G). This compares to the results of Oréal et al. [28] who described very faint expression of *cSox9* in day 6 gonads by *in situ* hybridization using sections. Our data demonstrate high levels of *cAmh* expression in day 6 male gonad, preceding the high levels of *cSox9* expression first detected in day 7 male gonad. They suggest that SOX9 is not responsible for the male-specific up-regulation of *cAmh*, but may play a role in the maintenance and/or amplification of *cAmh* expression in the male gonads once transcription is initiated. Our results support the previous observation that the male-specific high levels of *cAmh* expression precede testicular *cSox9* expression [28, 29].

We next examined expression of *Sox8*. At day 5, no *cSox8* expression was observed (fig. 1A). At day 6 and 7, *cSox8* expression was observed at the anterior tip of both male and female right gonads at similar levels (fig. 1B, C). This expression profile is different from that of *cAmh*, both in spatial distribution of transcripts and degree of sex specificity, suggesting that SOX8 could not be responsible for sex-specific up-regulation of *cAmh* in chicken.

The expression patterns of mouse and chicken *Sox8* imply that the functions of SOX8 are conserved in most but not all tissues between the two species. For example, *Sox8* is expressed in brain, skeletal muscle, eye, somite, dermomyotome, limb, digits, gut, spinal cord and dorsal root ganglia in both species [30, 31, 44]. However, some differences are evident in embryonic heart and gonad: in chicken, *cSox8* is expressed in the embryonic heart, testis and ovary, whereas in mouse, *Sox8* expression occurs predominantly in the embryonic testis, but not in the ovary or heart [31, 44]. Given these observations, SOX8 may contribute to the male-specific activation of *Amh* expression during gonadgenesis in mice but not chicken.

In mouse, only two SOX proteins, SOX8 and SOX9, have been identified as regulators of *Amh* expression in the embryonic gonad [26]. Based on our data, and previous studies [28, 29], neither SOX8 nor SOX9 can be responsible for the onset of high levels of *cAmh* expression

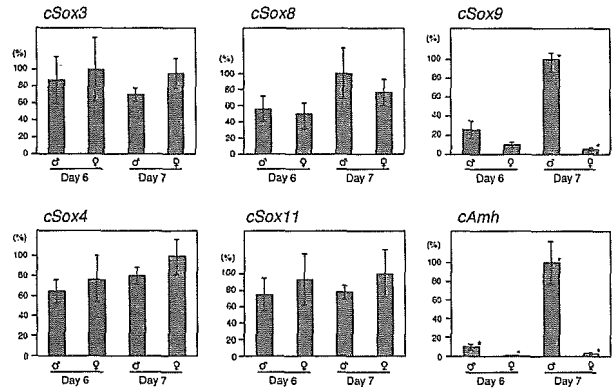

Figure 3. Quantitative, real-time RT-PCR analysis of *Sox* and *Amh* gene expression. Averages of three independent trials are shown as bars, with SEs shown as lines. Values marked with * were significantly different between males (♂) and females (♀) ($p = 0.0017$, 0.0047 and 0.012 for cSox9 at day 7, cAmh at day 6 and 7, respectively, using a two-sample equal variance t-test). Others were not significantly different between males and females ($p = 0.81$, 0.24, 0.74, 0.52, 0.17, 0.67, 0.38, 0.64, 0.49 for *cSox3* at day 6 and 7, *cSox8* at day 6 and 7, *cSox9* at day 6, *cSox4* at day 6 and 7, and *cSox11* at day 6 and 7, respectively).

in chicken, even though two SOX-binding sites are predicted in the *cAmh* promoter region. These observations prompted us to search for other *Sox* genes expressed in chicken male gonads that could be considered as candidate regulators of *Amh* expression. We conducted the analysis at day 6, since at this stage *cAmh* is expressed at high levels in male gonads while *cSox9* is either not expressed or expressed at a very low level.

We utilized degenerate RT-PCR on purified day 6 male gonad RNA using generic *Sry*-type HMG box primers to generate fragments for cloning into a plasmid vector. Twenty independent clones were sequenced, revealing that 12 clones were *cSox4* [45], 7 were *cSox11* [46] and 1 was *cSox9* [47].

One possible explanation for these results is that the degenerate primers used show a bias for amplification of *cSox4* and *cSox11* templates. To examine this possibility, we used the same degenerate primers to amplify *Sox* fragments from genomic DNA, in which all intronless *Sox* genes (Sox1, -2, -3, -4, -11, -12, -14, -21) capable of amplification by the primers are represented in equal proportions. Among ten clones amplified, none was *cSox4* or *cSox11*. Thus, primer bias does not explain our data relating to *cSox4* and *cSox11* expression in developing chicken gonads.

cSox4 and *cSox11* are expressed in male gonads at day 6, prompting us to examine the expression profiles of each in male and female gonads through the sex determination window. If both or either is expressed preferentially in male gonads, they could be considered a candidate for regulation of the *cAmh* gene. To evaluate the expression patterns of *cSox4* and *cSox11* in embryonic gonads, we employed whole-mount *in situ* hybridization analysis at the same stages previously used to profile *cSox8*, *cSox9* and *cAmh* expression. *cSox4* and *cSox11* signals were detected at similar levels in male and female gonads at all stages examined (fig. 2) suggesting that neither of them plays a role in sex-specific regulation of *Amh*.

The identification of *Sox* genes that are expressed in chicken embryonic gonads at day 5, 6 and 7 was previously attempted by McBride et al. [6]. Using RT-PCR amplification of the conserved *Sry*-type HMG box domain from RNA samples prepared from testes with mesonephroi attached, they found expression of *cSox3*, *cSox4*, *cSox9*, *cSox11*, *cSox12* and *cSox14*. Our data confirm that *cSox4*, *cSox9* and *cSox11* are indeed expressed, as is cSox3 (see below); however; we amplified the HMG box from day 6 gonad only, and this difference along with the differences in PCR primers, may explain the discrepancies in the data for *cSox12* and *cSox14*. Moreover, day 6 male gonad expresses *cSox4* and *cSox11* transcripts so abundantly that RT-PCR cloning is difficult for *Sox* genes expressed at low levels.

To examine the levels of gene expression quantitatively, we utilized RT-PCR and real-time RT-PCR analyses using RNAs isolated from pooled, sexed embryonic gonads at days 6 and 7 (fig. 3). As expected, *cAmh* and *cSox9* were expressed at different levels between males and females at day 7. At day 6, the expression levels of *cAmh* were statistically different between males and females ($p < 0.005$) while the expression levels of *cSox9* were not ($p > 0.1$). However, *cSox3*, *cSox4*, *cSox8* and *cSox11* were expressed at similar levels between males and females at days 6 and 7, suggesting that none of these *Sox* genes is responsible for the male-specific up-regulation of *cAmh* expression.

We were unable to amplify *cSox12* and *cSox14* sequences by RT-PCR from chicken embryonic gonads. As a positive control, chicken genomic DNA was included as template. Signals were observed at expected size of 108 bp for *cSox12* and 331 bp for *cSox14* only from genome template, but not from gonad RNA samples, showing that neither gene is expressed in embryonic gonads at day 6 and day 7 (data not shown).

Previous studies have eliminated *cSox3* as a candidate for male-specific up-regulation of *Amh* expression because *cSox3* is expressed at similar levels in the male and female gonads at the sex-determining window [28, 29]. Our present data support this conclusion. We rule out *cSox8* because it is expressed in a different spatial pattern to *Amh*, and *cSox12* and *-14* because they are not expressed in gonads at sex-determining stages at all. We exclude *cSox4* and *cSox11* also, on the basis of equivalent expression levels between male and female. It is formally possible that *cSox4* and *cSox11* might be expressed in Sertoli cells in the male (the site of *Amh* expression) and in another cell lineage in females, in which *Amh* is

not expressed, but we consider this unlikely, especially considering that all genes found to be involved in sex-specific development of the gonads to date show a sexually dimorphic pattern of gene expression in fetal gonads when examined by whole-mount *in situ* hybridization. However, one still cannot exclude the possibility of SOX protein-mediated regulation of *cAmh* gene expression, and further extensive cloning of *cSox* genes may be necessary to discover a *Sox* gene expressed predominantly in chicken embryonic testis.

Alternatively, we have to consider that sex-specific *Amh* up-regulation is not mediated by SOX proteins in birds. Even though the putative SF1-binding site, like the two SOX-binding site in the *Amh* promoter, is conserved between mouse and chicken [28], and *cSf1* is co-expressed with *cAmh* at day 7 of chicken embryonic testis [15], the expression profiles of mouse and chicken *Sf1* show major differences. Before testis cord formation, *Sf1* is expressed at similar levels in males and females in both species, while subsequently, chicken *Sf1* expression is maintained in the testis, but is up-regulated in the ovary [12, 15, 29]. The opposite expression pattern is reported for mouse *Sf1* [reviewed in ref. 48]. This difference could be explained by the possibility that *SF1* functions in more steroidogenically active tissue (testis in mammals and ovary in birds), or that *Sf1* may not be associated with testis formation in birds [12]. Either way, the expression profile of *cSf1*, like that of *cSox9* [28] and *cSox8* (this study), suggests that it is not responsible for male-specific up-regulation of *cAmh* expression during chicken gonad genesis. Since both SF1 and SOX proteins are required for normal levels of *Amh* expression during sex determination in mouse [27], this may imply that there is a different mechanism of *cAmh* regulation in chicken compared with mouse, and that SOX protein is not a causative factor for sex-specific expression of *cAmh*.

Gonadal expression of *Sox8*, which has an evolutionarily conserved coding protein among vertebrates, has been studied in mouse, chicken and red-eared slider turtle [31, 49]. *Sox8* is expressed in the developing testes of all three species, implying a functional significance, but in chicken and turtle, *Sox8* is also expressed in the ovary. So far, up-regulation of mouse *Amh* is the only known molecular function for the SOX8 protein [26]. If this function is conserved among vertebrates, chicken SOX8 may have a protein partner which is expressed in males to activate or in females to suppress *cAmh*. Some genes are expressed sex specifically during gonadal differentiation in the mouse, including *Sf1* [13], *Wt1* [50], *Gata4* [14], *Lhx9* [51], *Wnt-4* [52] and *Dax1* [53]. However, chicken homologues of these genes are not candidates because they are expressed in both developing testis and ovary while *cAmh* is differentially expressed [15, 29]. *Dmrt1* is expressed only in developing testis in mouse, while chicken *Dmrt1* is expressed in both developing gonads with higher levels in testis, suggesting that it is not such a factor [15, 54]. The identification of a chicken SOX8-binding partner may clarify this possibility. Finally, further analysis of the *cAmh* promoter may reveal whether SOX proteins play a role in its up-regulation, and whether similarities exist in the mechanisms that regulate *Amh* expression in birds and mammals.

Acknowledgements. We thank M. Hargrave, K. Loffler and J. Bowles and members of the Koopman laboratory for technical advice and constructive criticism, and D. Wilhelm and F. Martinson for critical reading of this manuscript. P. K. is a Professorial Research Fellow of the Australian Research Council.

1 Gubbay J., Collignon J., Koopman P., Capel B., Economou A., Münsterberg A. et al. (1990) A gene mapping to the sex-determining region of the mouse Y chromosome is a member of a novel family of embryonically expressed genes. Nature **346:** 245–250
2 Sinclair A. H., Berta P., Palmer M. S., Hawkins J. R., Griffiths B. L., Smith M. J. et al. (1990) A gene from the human sex-determining region encodes a protein with homology to a conserved DNA-binding motif. Nature **346:** 240–244
3 Koopman P., Gubbay J., Vivian N., Goodfellow P. and Lovell-Badge R. (1991) Male development of chromosomally female mice transgenic for Sry. Nature **351:** 117–121
4 Coriat A.-M., Muller U., Harry J. L., Uwanogho D. and Sharpe P. T. (1993) PCR amplification of SRY-related gene sequences reveals evolutionary conservation of SRY-box Motif. PCR Methods Appl. **2:** 218–222
5 Griffiths R. (1991) The isolation of conserved DNA sequences related to the human sex determing region Y gene from the lesser black-backed gull (Larus fuscus). Proc. R. Soc. Lond. B. **224:** 123–128
6 McBride D., Sang H. and Clinton M. (1997) Expression of Sry-related genes in the developing genital ridge/mesonephros of the chick embryo. J. Reprod. Fertil. **109:** 59–63
7 Tiersch T. R., Mitchell M. J. and Wachtel S. S. (1991) Studies on the phylogenetic conservation of the SRY gene. Hum. Genet. **87:** 571–573
8 Clinton M. (1998) Sex determination and gonadal development: a bird's eye view. J. Exp. Zool. **281:** 457–465
9 Carré-Eusèbe D., Clemente N. di, Rey R., Pieau C., Vigier B., Josso N. et al. (1996) Cloning and expression of the chick anti-Müllerian hormone gene. J. Biol. Chem. **271:** 4798–4804
10 Morais da Silva S., Hacker A., Harley V., Goodfellow P., Swain A. and Lovell-Badge R. (1996) Sox9 expression during gonadal development implies a conserved role for the gene in testis differentiation in mammals and birds. Nat. Genet. **14:** 62–68
11 Kent J., Wheatley S. C., Andrews J. E., Sinclair A. H. and Koopman P. (1996) A male-specific role for SOX9 in vertebrate sex determination. Development **122:** 2813–2822
12 Smith C. A., Smith M. J. and Sinclair A. H. (1999b) Expression of chicken steroidogenic factor-1 during gonadal sex differentiation. Gen. Comp. Endocrinol. **113:** 187–196
13 Ikeda Y., Shen W. H., Ingraham H. A. and Parker K. L. (1994) Developmental expression of mouse steroidogenic factor-1, an essential regulator of the steroid hydroxylases. Mol. Endocrinol. **8:** 654–662
14 Viger R. S., Mertineit C., Trasler J. M. and Nemer M. (1998) Transcription factor GATA-4 is expressed in a sexually dimorphic pattern during mouse gonadal development and is a potent activator of the Müllerian inhibiting substance promoter. Development **125:** 2665–2675
15 Oréal E., Mazaud S., Picard J.-Y., Magre S. and Carré-Eusèbe D. (2002) Different patterns of anti-Müllerian hormone expres-

sion, as related to DMRT1, SF-1, WT1, GATA-4, Wnt-4, and Lhx9 expression, in the chick differentiating gonads. Dev. Dyn. **225:** 221–232
16 Wegner M. (1999) From head to toes: the multiple facets of Sox proteins. Nucleic Acids Res. **15:** 1409–1420
17 Bowles J., Schepers G. and Koopman P. (2000) Phylogeny of the SOX family of developmental transcription factors based on sequence and structural indicators. Dev. Biol. 227: 239–255
18 Schepers G. E., Teasdale R. D. and Koopman P. (2002) Twenty pairs of Sox: extent, homology, and nomenclature of the mouse and human sox transcription factor gene families. Dev. Cell. **3:** 167–170
19 Foster J. W., Dominguez-Steglich M. A., Guioli S., Kowk C., Weller P. A., Weissenbach J. et al. (1994) Campomelic dysplasia and autosomal sex reversal caused by mutations in an SRY-related gene. Nature **372:** 525–30
20 Wagner T., Wirth J., Meyer J., Zabel B., Held M., Zimmer J. et al. (1994) Autosomal sex reversal and campomelic dysplasia are caused by mutations in and around the SRY-related gene SOX9. Cell **79:** 1111–120
21 Vidal V. P. I., Chaboissier M.-C., Rooij D. G. de and Schedl A. (2001) Sox9 induces testis development in XX transgenic mice. Nat. Genet. **28:** 216–17
22 Josso N., Clemente N. di and Gouédard L. (2001) Anti-Müllerian hormone and its receptors. Mol. Cell. Endocrinol. **179:** 25–32
23 Nachtigal M. W., Hirokawa Y., Enyeart-VanHouten D. L., Flanagan J. N., Hammer G. D. and Ingraham H. A. (1998) Wilms' tumor 1 and Dax-1 modulate the orphan nuclear receptor SF-1 in sex-specific gene expression. Cell **93:** 445–454
24 Tremblay J. J. and Viger R. S. (1999) Transcription factor GATA-4 enhances Müllerian inhibiting substance gene transcription through a direct interaction with the nuclear receptor SF-1. Mol. Endocrinol. **13:** 1388–1401
25 Santa Barbara P. de, Bonneaud N., Boizet B., Desclozeaux M., Moniot B., Südbeck P. et al. (1998) Direct interaction of SRY-related protein SOX9 and steroidogenic factor 1 regulates transcription of the human anti-Müllerian hormone gene. Mol. Cell. Biol. **18:** 6653–6665
26 Schepers G., Wilson M., Wilhelm D. and Koopman P. (2003) SOX8 is expressed during testis differentiation in mice and synergizes with SF1 to activate the Amh promoter in vitro. J. Biol. Chem. **278:** 28101–28108
27 Arango N. A., Lovell-Badge R. and Behringer R. R. (1999) Targeted mutagenesis of the endogenous mouse Mis gene promoter: in vivo definition of genetic pathways of vertebrate sexual development. Cell **99:** 409–419
28 Oréal E., Pieau C., Mattei M. G., Josso N., Picard J.-Y., Carré-Eusèbe D. et al. (1998) Early expression of AMH in chicken embryonic gonads precedes testicular SOX9 expression. Dev. Dyn. **212:** 522–532
29 Smith C. A., Smith M. J. and Sinclair A. H. (1999a) Gene expression during gonadogenesis in the chicken embryo. Gene **234:** 395–402
30 Takada S. and Koopman P. (2003) Origin and possible roles of the Sox8 transcription factor gene during sexual development. Cytogenet. Genome Res. **101:** 212–218
31 Schepers G. E., Bullejos M., Hosking B. M. and Koopman P. (2000) Cloning and characterisation of the Sry-related transcription factor gene Sox8. Nucleic Acids Res. **28:** 1473–1480
32 Wright E., Hargrave M. R., Christiansen J., Cooper L., Kun J., Evans T. et al. (1995) The Sry-related gene Sox-9 is expressed during chondrogenesis in mouse embryos. Nat. Genet. **9:** 15–20
33 Pusch C., Hustert E., Pfeifer D., Südbeck P., Kist R., Roe B. et al. (1998) The SOX10/Sox10 gene from human and mouse: sequence, expression, and transactivation by the encoded HMG domain transcription factor. Hum. Genet. **103:** 115–123
34 Collignon J., Sockanathan S., Hacker A., Cohen-Tannoudji M., Norris D., Rastan S. et al. (1996) A comparison of the properties of Sox-3 with Sry and two related genes, Sox-1 and Sox-2. Development **122:** 509–520
35 Smits P., Li P., Mandel J., Zhang Z., Deng J. M., Behringer R. R. et al. (2001) The transcription factors L-Sox5 and Sox6 are essential for cartilage formation. Dev Cell **1:** 277–290
36 Downes M. and Koopman P. (2001) SOX18 and the transcriptional regulation of blood vessel development. Trends Cardiovasc. Med. **11:** 318–324
37 Kanai-Azuma M., Kanai Y., Gad J. M., Tajima Y., Taya C., Kurohmaru M. et al. (2002) Depletion of definitive gut endoderm in Sox17-null mutant mice. Development **129:** 2367–2379
38 Pennisi D., Bowles J., Nagy A., Muscat G. and Koopman P. (2000) Mice null for Sox18 are viable and display a mild coat defect. Mol. Cell. Biol. **20:** 9331–9336
39 Hamburger V. and Hamilton H. L. (1951) A series of normal stages in the development of the chick embryo. J. Morphol. **88:** 49–92
40 Clinton M., Haines L., Belloir B. and McBride D. (2001) Sexing chick embryos: a rapid and simple protocol. Br. Poult. Sci. **42:** 134–138
41 Chomczynski P. and Sacchi N. (1987) Single-step method of RNA isolation by acid guanidinium thiocyanate-phenol-chloroform extraction. Anal. Biochem. **162:** 156–159
42 Xu Q. and Wilkinson D. (1998) In situ hybridization of mRNA with hapten labelled probes. In: In Situ Hybridization: a Practical Approach, 2nd ed., pp. 87–106, Wilkinson D. (ed.), Oxford University Press, Oxford
43 Romanoff A. L. (1960) The Avian Embryo: Structural and Functional Development, Macmillan, New York
44 Bell K. M., Western P. S. and Sinclair A. H. (2000) SOX8 expression during chick embryogenesis. Mech. Dev. 94: 257–260
45 Maschhoff K. L., Anziano P. Q., Ward P. and Baldwin H. S. (2003) Conservation of Sox4 gene structure and expression during chicken embryogenesis. Gene **320:** 23–30
46 Uwanogho D., Rex M., Cartwright E. J., Pearl G., Healy C., Scotting P. J. et al. (1995) Embryonic expression of the chicken Sox2, Sox3 and Sox11 genes suggests an interactive role in neuronal development. Mech. Dev. **49:** 23–36
47 Healy C, Uwanogho D. and Sharpe P. T. (1999) Regulation and role of Sox9 in cartilage formation. Dev. Dyn. **215:** 69–78
48 Parker K. L. and Schimmer B. P. (1997) Steroidogenic factor 1: a key determinant of endocrine development and function. Endocr. Rev. **18:** 361–377
49 Takada S., DiNapoli L., Capel B. and Koopman P. (2004) Sox8 is expressed at similar levels in gonads of both sexes during the sex determining period in turtles. Dev. Dyn. **231:** 387–395
50 Pelletier J., Schalling M., Buckler A. J., Rogers A., Haber D. A. and Housman D. (1991) Expression of the Wilms' tumor gene WT1 in the murine urogenital system. Genes. Dev. **5:** 1345–1356
51 Birk O. S., Casiano D. E., Wassif C. A., Cogliati T., Zhao L., Zhao Y. et al. (2000) The LIM homeobox gene Lhx9 is essential for mouse gonad formation. Nature **403:** 909–913
52 Vainio S., Heikkila M., Kispert A., Chin N. and McMahon A. P. (1999) Female development in mammals is regulated by Wnt-4 signalling. Nature **397:** 405–409
53 Swain A., Zanaria E., Hacker A., Lovell-Badge R. and Camerino G. (1996) Mouse Dax1 expression is consistent with a role in sex determination as well as in adrenal and hypothalamus function. Nat. Genet. **12:** 404–409
54 Raymond C. S., Kettlewell J. R., Hirsch B., Bardwell V. J. and Zarkower D. (1999) Expression of Dmrt1 in the genital ridge of mouse and chicken embryos suggests a role in vertebrate sexual development. Dev. Biol. **215:** 208–220

Available online at www.sciencedirect.com
SCIENCE DIRECT®
Journal of Steroid Biochemistry & Molecular Biology 96 (2005) 1–12
The Journal of Steroid Biochemistry & Molecular Biology
www.elsevier.com/locate/jsbmb

Transcriptional repression of fibroblast growth factor 8 by transforming growth factor-β in androgen-dependent SC-3 cells

Norio Takayashiki, Hirotoshi Kawata, Tomoko Kamiakito, Akira Tanaka *

Department of Pathology, Jichi Medical School, 3311-1 Yakushiji, Minamikawachi, Kawachi, Tochigi 329-0498, Japan

Received 5 July 2004; accepted 10 January 2005

Abstract

We here characterized the transcriptional profiles of TGF-β-responsive genes using androgen-dependent mouse mammary carcinoma SC-3 cells. Compared with the testosterone-stimulated SC-3 cells, 165 genes were up-regulated at more than 5-fold, and 78 genes were down-regulated to less than one-third in response to TGF-β. Of note, *fgf8*, an androgen-inducible growth factor essential to the androgen-dependent growth of SC-3 cells, was severely repressed in response to TGF-β. Real-time PCR confirmed that the androgenic induction of the *fgf8* transcripts is severely attenuated by TGF-β. Although a considerable number of growth-suppressive genes were up-regulated in response to TGF-β, the treatment with TGF-β was insufficient to lead SC-3 cells to apoptosis within 24 h by both the TUNEL method and the caspase 3 activity assay. Flow cytometric analysis rather indicated the cell-static effect of TGF-β on the androgen-stimulated SC-3 cells. In addition, TGF-β failed to suppress the FGF8-stimulated growth of SC-3 cells, suggesting that the repression of *fgf8* is required for the TGF-β-mediated growth inhibition in SC-3 cells. In a reporter assay, androgen-responsive promoter activity was suppressed by TGF-β in SC-3 cells. Based on this finding, it is likely that some of the androgen-inducible genes are physiological targets of the TGF-β-mediated transcriptional control, and therefore, it is strongly suggested that the repression of *fgf8* might be directly or indirectly involved in this transcriptional control by TGF-β.

Keywords: FGF8; TGF-β; Androgen; Oligonuceotide microarray

Transforming growth factor (TGF)-β is a multifunctional peptide growth factor involving various physiological and pathological cellular responses. In general, TGF-β serves as an inhibitor of cell growth [1]. The TGF-β signals are transduced into the nucleus through Smad proteins, resulting in the transcriptional activation of growth-inhibitory genes. For instance, $p15^{INK4B}$, one of the cyclin-dependent kinase inhibitors (CDKIs), is activated in response to TGF-β in cancer cells, leading to growth arrest [2,3]. In contrast, recent reports have shown that TGF-β is also involved in cancer progression mainly through the epithelial–mesenchymal transition (EMT) [4], known as a phenomenon in which cancer cells acquire more aggressive and invasive phenotypes than before by loosing epithelial gene expressions and gaining mesenchymal ones. In addition, TGF-β facilitates the expressions of extracellular matrix proteins and matrix remodeling proteins [5], also supporting the cancer invasion. Thus, the functions of TGF-β seem to be considerably varied among cancer cells.

An androgen-dependent mouse mammary carcinoma SC-3 cell line is one of the best in vitro models for understanding the growth mechanism of human hormone-responsive cancers. Our earlier reports have clearly demonstrated that *fgf8* plays an essential role in the androgen-dependent growth of SC-3 cells [7], and that FGF8 is involved in the growth of human prostate and breast cancers [8–10]. In our previous report, it was also demonstrated that TGF-β suppresses the androgen-dependent growth of SC-3 cells [11], indicating that SC-3 cells preserve the TGF-β signaling. Recently, it has been reported that the transcription of an androgen-regulated prostate-specific antigen (PSA) gene is repressed by the overexpression of *Smad3* [6], suggesting that TGF-β signals are involved in the transcriptional control of androgen-regulated genes in a repressive manner. This finding prompted us to investigate TGF-β-responsive genes in SC-3 cells using an oligonucleotide microarray method. In this analysis, *fgf8* was

* Corresponding author. Tel.: +81 285 58 7330; fax: +81 285 44 8467.
E-mail address: atanaka@jichi.ac.jp (A. Tanaka).

0960-0760/$ – see front matter © 2005 Elsevier Ltd. All rights reserved.
doi:10.1016/j.jsbmb.2005.01.031

by far the most markedly regulated gene in response to TGF-β. We further investigated the roles of the transcriptional repression of *fgf8* in TGF-β-mediated growth arrest in SC-3 cells.

1. Materials and methods

1.1. Cells

The SC-3 cells used in this study were established from an SC115 tumor. The method for cloning and the culture conditions were described previously [7]. For the establishment of stably FGF8-expressing SC-3 cells, pKANTEX93-FGF8 plasmid, kindly gifted from Dr. Shitara at Kyowa Hakko Kogyo, was transfected into SC-3 cells, and stably FGF8-expressing SC-3 cells were isolated.

1.2. Cell growth

The method for the MTT assay was described previously [9]. Briefly, SC-3 cells were plated onto a 96-well plate (3×10^3 per well) in a serum-free basal medium (DMEM:Ham's F-12 (1:1, v/v)), supplemented with 2% fetal bovine serum (FBS) treated with dextran-coated charcoal (dcc). The next day, the cells were stimulated with 50 ng/ml recombinant mouse FGF8 (R&D Systems, Minneapolis, MN, USA) in the presence or absence of various concentrations of recombinant human TGF-β1 (R&D Systems) under the serum-free condition. After 72 h of further incubation, MTT was added to the medium at a final concentration of 1 mg/ml. After another 4-h incubation, formazan substrates were collected, resolved with DMSO, and then measured at an absorbance of 570 nm, with reference at 690 nm.

1.3. RNAs

SC-3 cells were plated onto 100 mm-dishes (1.0×10^6 cells/dish) in a basal medium supplemented with 2% dcc-treated FBS under an androgen-free condition. The next day, the cells were stimulated with 10 nM testosterone in the presence or absence of 10 ng/ml TGF-β1 under the serum-free condition. Total cellular RNAs were prepared by an acid guanidium isothiocyanate–phenol–chloroform method at 12 h for the oligonucleotide microarray analysis. For the real-time PCR, total cellular RNAs were prepared using an RNeasy Kit (Qiagen GmbH, Hilden, Germany) at 0, 6, 12 and 24 h. Poly (A) RNAs were purified using the Oligotex-dT30 mRNA Purification Kit (TAKARA Biochemicals, Kyoto, Japan).

1.4. Oligonucleotide microarray analysis

The oligonucleotide microarray analysis was performed using a murine genome GeneChip U74A array (Affymetrix, Santa Clara, CA, USA) according to the standard protocols supplied by Affymetrix. Briefly, double-stranded cDNAs were synthesized from 1 μg of poly (A) RNA using the Superscript Choice System (Invirtogen, Carlsbad, CA, USA), then biotin-labeled cRNAs were prepared from these synthesized cDNAs by an RNA Transcript Labeling Kit (Enzo Life Sciences, Farmingdale, NY, USA). The fragmented cRNAs were hybridized with the U74A array for 16 h at 45 °C and 60 rpm. The array was washed on a GeneChip Fluidics Station 400 (Affymetrix) using an automated program, and the signals were then detected by a GMS 418 array scanner (Affymetrix). Scanned outputs were analyzed by Affymetrix software. Although the background levels were below 100, genes showing values lower than 200, either after the induction of TGF-β-inducible genes or before the repression of TGF-β repressive genes, were excluded because of their marginal expression.

1.5. Real-time PCR

Single-stranded cDNAs were synthesized using Superscript III (Invitrogen) according to the manufacturer's instructions from 1 μg of total cellular RNAs using an oligo dT primer. The PCR products were monitored by an ABI PRISM 7700 (Applied Biosystems, Foster City, CA, USA) using TaqMan probes. Primer sets used here were: mouse *fgf8*, 5′-CTGCTGTTGCACTTGCTGGT-3′ (forward primer); 5′-TCCCTCACATGCTGTGTAAAATTAG-3′ (reverse primer); Fam-CTCTGCCTCCAAGCCCAGGTAACTGTT-Tamra (TaqMan probe); mouse prostate stem cell antigen (PSCA), 5′-GGCTGAGATGGGATGGACTG-3′ (forward primer); 5′-CTGGGACTCCTGGTGCCTC-3′ (reverse primer); Fam-CAGAAATGGAGCTGGGAGGTGGGTG-Tamura (TaqMan probe); mouse lipocalin 7, 5′-GGAGGA-CAGTCGCGTACACA-3′ (forward primer); 5′-TGCCTCC-TGGAGTAGCCCTT-3′ (reverse primer); Fam-TGTCCTT-AAGCCGTTCCCTCGGAGC-Tamra (TaqMan probe); mouse β-actin, 5′-AGTGTGACGTTGACATCCGTAAAG-3′ (forward primer); 5′-AATGCCTGGGTACATGGTGGTA-3′ (reverse primer); and Fam-CCTCTATGCCAACAC-AGTGTTGTCTGGTG-Tamra (TaqMan probe).

1.6. Detection of apoptosis

The caspase 3 activity was measured using a Caspase 3 Assay Kit (Sigma–Aldrich, St. Louis, MO, USA). Briefly, SC-3 cells (2.5×10^6 cells/dish) were plated and stimulated with 10 nM testosterone in the presence or absence of 10 ng/ml TGF-β1 or 5 ng/ml recombinant mouse tumor necrosis factor (TNF)-α (PeproTech Inc., Rocky Hill, NJ, USA) for the indicated hours under a serum-free condition. The cell lysates were collected and suspended in the lysis buffer from the kit. After removal of the cell debris by centrifuguration, the peptide substrate acetyl-Asp-Glu-val-Asp-*p*-nitroanilide (Ac-DEVD-pNA) was added to the aliquots. After incubation for 2 h at 37 °C, the samples were measured at an absorbance of 405 nm.

Apoptosis was also evaluated by the TUNEL method using an ApopTag Peroxidase In Situ Apoptosis Detection Kit (CHEMICON Interntional, Temecula, CA, USA). Briefly, SC-3 cells were plated onto 4-well-chamber slides, and then the cells were treated with test compounds for the indicated hours. After fixation with 1% paraformaldehyde (pH 7.4) for several hours at 4 °C, the slides were washed and the nucleotide nick ends were tailed with digoxigenin-dNTPs using terminal deoxynucleotidyl transferase (TdT) for 1 h at 37 °C. The slides were then incubated with an anti-digoxigenin antibody conjugated to peroxidase, and immunostained with 3,3′-diaminobenzidine tetrahydrochloride. Positive cells per one hundred cells were counted in four different areas on each slide.

Table 1
Top 40 of TGF-β-inducible genes in androgen-stimulated SC-3 cells

No.	Genbank accession	Gene symbol	Gene name	Microarray data		
				T[a]	+TGF-β[b]	Ratio
1	X91617	Xrn1	5′–3′ Exoribonuclease 1	4.9	258.4	52.7
2	AW125043	C820004H04Rik	RIKEN cDNA C820004H04 gene	15.4	588	38.2
3	X05546	Ccrn4l	CCR4 carbon catabolite repression 4-like (*S. cerevisiae*)	367.3	13059	35.6
4	M58564	Zfp36l2	Zfp36l2: zinc finger protein 36, C3H type-like 2	8.7	274.1	31.5
5	Y17793	Robo1	Roundabout homolog 1 (*Drosophila*)	7.6	204.2	26.9
6	AA797843	D11Ertd530e	DNA segment, Chr 11, ERATO Doi 530, expressed	11.8	269.1	22.8
7	AB010383	Ror1	Receptor tyrosine kinase-like orphan receptor 1	16.1	359.3	22.3
8	AW060401	Arhq	ras homolog gene family, member Q	96.2	1957.8	20.4
9	X07888		*M. musculus* HMGCR gene for 3-hydroxy-3-methylglutaryl coenzyme A reductase, exon 2	18.4	360.3	19.6
10	AF002823	Bub1	Budding uninhibited by benzimidazoles 1 homolog (*S. cerevisiae*)	12.4	235.9	19.0
11	AW228840		up22f10.x1 NCI_CGAP_Mam2 Mus musculus cDNA clone, IMAGE:2655115 3′, MRNA sequence	15.6	285.5	18.3
12	AW046027	2010204I15Rik	RIKEN cDNA 2010204I15 gene	13.2	220.9	16.7
13	X57349	Trfr	transferrin receptor	16.9	280.5	16.6
14	AF076845	Hus1	Hus1 homolog (*S. pombe*)	22.7	369.2	16.3
15	AV003873	Clu	Clusterin	15.9	257.3	16.2
16	AW045443	Mef2a	Myocyte enhancer factor 2A	44.3	702.4	15.9
17	X53250	Zfa	Zinc finger protein, autosomal	15.9	251.1	15.8
18	D50032	Tgoln2	*trans*-Golgi network protein 2	16.2	253.9	15.7
19	AB035174	Siat7f	Sialytransferase 7 ((alpha-*N*-acetylneuraminyl 2,3-betagalactosyl-1,3)-*N*-acetyl galactosaminide alpha -2,6-sialytransferase) F	15.6	234.4	15.0
20	AF100777	Wisp1	WNT1-inducible signaling pathway protein 1	72.3	1080.2	14.9
21	M60474	Marcks	Myristoylated alanine rich protein kinase C substrate	59.7	873.4	14.6
22	AI848924	Parg	Poly (ADP-ribose) glycohydrolase	29.2	418.7	14.3
23	D86603	Bach1	BTB and CNC homology 1	15.8	220.4	13.9
24	D12713		Mus musculus gene for MSEC66, complete cds	25.1	326.8	13.0
25	D26532	Runx1	Runt related transcription factor 1	62.9	788	12.5
26	AV138783	Gadd45b	Growth arrest and DNA-damage-inducible 45 beta	62.7	779.3	12.4
27	AF084480	Baz1b	Bromodomain adjacent to zinc finger domain, 1B	20.2	242.8	12.0
28	U68182	Gcnt2	Glucosaminyltransferase, I-branching enzyme	40.8	440.4	10.8
29	AI642553	Iqgap1	IQ motif containing GTPase activating protein 1	47.7	503.8	10.6
30	AI839116	2310034L04Rik	RIKEN cDNA 2310034L04 gene	47.3	497.8	10.5
31	X57349	Trfr	Transferrin receptor	54	557.1	10.3
32	AV380793	Eif4g1	Eukaryotic translation initiation factor 4, gamma 1	97.3	964.4	9.9
33	AF000294	Pparbp	Peroxisome proliferator activated receptor binding protein	40.7	399.8	9.8
34	AW214136		uo40c11.x1 NCI_CGAP_Lu29 Mus musculus cDNA clone IMAGE:2645012 3′ Similar to TR: O89815 O89815 POL POLYPROTEIN, MRNA sequence	142.8	1362.2	9.5
35	AJ238636	Entpd5	Ectonucleoside triphosphate diphosphohydrolase 5	22.4	210.1	9.4
36	AA763004		Mus musculus cDNA clone IMAGE:6331951, partial cds	147.1	1373.2	9.3
37	X57349	Trfr	Transferrin receptor	46.2	425.3	9.2
38	U14135	Itgav	Integrin alpha V	27.2	249.1	9.2
39	U73478	Anp32a	Acidic (leucine-rich) nuclear phosphoprotein 32 family, member A	239.9	2167.7	9.0
40	D87900	Arf3	ADP-ribosylation factor 3	45	406.3	9.0

[a] T, 10 nM testosterone
[b] +TGF-β, 10 nM testosterone plus 10 ng/ml of recombinant human TGF-β1.

1.7. Flow cytometry

SC-3 cells were plated onto 100 mm-dishes (1.0×10^6 cells/dish) in a protein-free basal medium under an androgen-free condition for synchronization at G1 phase. After incubation for 24 h, the cells were untreated or treated with 10 nM testosterone in the presence or absence of 10 ng/ml TGF-β1 in a serum-free basal medium containing 0.1% bovine serum albumin. At indicated hours, the cells were collected by a cell-scraper, and fixed with 1% paraformaldehyde. The cells were stained with propiodium iodide in a sodium citrate buffer containing 0.1% NP-40 and 10 μg/ml RNase. Then, DNA contents were measured by a BD LSR (BD Biosciences, San Jose, CA, USA).

1.8. Luciferase assay

The nucleotide sequences of the promoter regions for human PSCA (~3.0 kbp) and PSA (~0.55 kbp) were isolated from the database at http://dbtss.hgc.jp, and amplified by genomic PCR. After confirmation of the nuceotide sequencing, the amplified genomic DNAs were subcloned into a pGL-3 luciferase vector (Promega, Madison, WI, USA). The core promoter region of the *fgf8* gene (~0.3 kbp), previously iso-

Table 2
Top 40 of TGF-β-repressive genes in androgen-stimulated SC-3 cells

No.	Genbank accession	Gene symbol	Gene name	Microarray data		
				T[a]	+TGF-β[b]	Ratio
1	D12483	Fgf8	Fibroblast growth factor 8	1620.4	20.5	0.01
2	M32032	Selenbp1	Selenium binding protein 1	535.4	14.8	0.03
3	K02588	Cyp1a1	Cytochrome P450, family 1, subfamily a, polypeptide 1	2384.9	85.9	0.04
4	M17979		Mouse epidermal growth factor binding protein type 1 gene, exons 3–5	264	12.8	0.05
5	J00389	Klk26	Kallikrein 26	212.5	20.2	0.10
6	X15662	Krt2–8	Keratin complex 2, basic, gene 8	627.8	60.7	0.10
7	AF045887	Agt	Angiotensinogen	1201.4	123	0.10
8	AV089850	Aldh3a1	Aldehyde dehydrogenase family 3, subfamily A1	2836.2	323.9	0.11
9	AW049768	Lcn7	Lipocalin 7	6025.2	726.9	0.12
10	D16215	Fmo1	Flavin containing monooxygenase 1	249.4	33.3	0.13
11	AF044030	Ltb4r1	Leukotriene B4 receptor 1	343.1	46.3	0.13
12	AF017128	Fosl1	fos-like antigen 1	5166.2	724.9	0.14
13	AF019385	Hs3st1	Heparan sulfate (glucosamine) 3-O-sulfotransferase 1	648.7	96.1	0.15
14	U07634	Epha2	Eph receptor A2	948.2	147.9	0.16
15	U62674		Mus musculus histone H2a.2–615 (H2a-615), and histone H3.2–615 (H3-615) genes, complete cds	4384.4	725.3	0.17
16	L06047	Gsta4	Glutathione S-transferase, alpha 4	1804.1	309.2	0.17
17	M33988	Pdhb	Pyruvate dehydrogenase (lipoamide) beta	12993	2398	0.18
18	AI326288	Chrne	Cholinergic receptor, nicotinic, epsilon polypeptide	763.9	142.1	0.19
19	M10114	Csnk	Casein kappa	976.9	186.3	0.19
20	M64086	Serpina3n	Serine (or cysteine) proteinase inhibitor, clade A, member 3N	225.7	45	0.20
21	AA590358	2200008D09Rik	RIKEN cDNA 2200008D09 gene	749.3	150.7	0.20
22	D87896	Gpx4	Glutathione peroxidase 4	3747.8	780.8	0.21
23	U44088	Phlda1	Pleckstrin homology-like domain, family A, member 1	2418.4	515.7	0.21
24	U51743	Tead4	TEA domain family member 4	1168.5	252	0.22
25	AW048233	Erf	Ets2 repressor factor	2152.7	476	0.22
26	X78545	Mcpt8	Mast cell protease 8	356.1	78.8	0.22
27	M60523	Idb3	Inhibitor of DNA binding 3	621.5	138.8	0.22
28	AI843448	Mgst3	Microsomal glutathione *S*-transferase 3	3765.3	841	0.22
29	AF090686	Tcn2	Transcobalamin 2	224.7	50.6	0.23
30	AW209486	Psca	Prostate stem cell antigen	505.3	114	0.23
31	Y17709	Fzd9	Frizzled homolog 9 (*Drosophila*)	286.6	65.7	0.23
32	AF064984	Lrp5	Low density lipoprotein receptor-related protein 5	657.2	154.9	0.24
33	U51743	Tead4	TEA domain family member 4	2410.9	575.7	0.24
34	AI845584	Dusp6	Dual specificity phosphatase 6	3317.2	795.5	0.24
35	X61800	Cebpd	CCAAT/enhancer binding protein (C/EBP), delta	7501	1816	0.24
36	L09192	Pcx	Pyruvate carboxylase	1147.3	282	0.25
37	AA241764	Gstm5	Glutathione S-transferase, mu 5	209.9	52	0.25
38	AW047343	Dbp	D site albumin promoter binding protein	335.8	83.3	0.25
39	U88325	Socs1	Suppressor of cytokine signaling 1	1378.8	342.6	0.25
40	U14556	Zfp100	Zinc finger protein 100	318.9	79.4	0.25

[a] T, 10 nM testosterone.
[b] +TGF-β, 10 nM testosterone plus 10 ng/ml of recombinant human TGF-β1.

Table 3
Summary of upregulated genes by TGF-β in androgen-stimulated SC-3 cells

Genbank accession	Gene symbol	Description	Microarray data		
			T[a]	+TGF-β[b]	Ratio
Signal transduction molecule					
AW060401	Arhq	ras homolog gene family, member Q	96.2	1957.8	20.4
AI642553	Iqgap1	IQ motif containing GTPase activating protein 1	47.7	503.8	10.6
X83506	Utrn	Utrophin	29.3	216.2	7.4
D16250	Bmpr1a	Bone morphogenetic protein receptor, type 1A	39.9	294	7.4
U58513	Rock2	Rho-associated coiled-coil forming kinase 2	55.2	354.3	6.4
AW120511	Fbxw7	F-box and WD-40 domain protein 7, archipelago homolog (*Drosophila*)	34.4	216.5	6.3
M89802	Wnt7b	Wingless-related MMTV integration site 7B	243.9	1447.4	5.9
U50413	Pik3r1	Phosphatidylinositol 3-kinase, regulatory subunit, polypeptide 1 (p85 alpha)	47.7	278.9	5.8
U64828	Ncoa1	Nuclear receptor coactivator 1	38	216	5.7
AW060819	Twsg1	Twisted gastrulation homolog 1 (*Drosophila*)	116	627.8	5.4
AI846922	Rasa1	RAS p21 protein activator 1	113.4	594.1	5.2
AF071312	Cops2	COP9 (constitutive photomorphogenic) homolog, subunit 2 (*Arabidopsis thaliana*)	73.9	372.6	5.0
Cytokine, growth factor or growth factor ligand					
D16250	Bmpr1a	Bone morphogenetic protein receptor, type 1A	39.9	294	7.4
M95200	Vegfa	Vascular endothelial growth factor A	158.6	1003.2	6.3
X54542	Il6	Interleukin 6	35.7	203	5.7
Transcriptional factor or modulator					
AA797843	D11Ertd530e	DNA segment, Chr 11, ERATO Doi 530, expressed	11.8	269.1	22.8
AW045443	Mef2a	Myocyte enhancer factor 2A	44.3	702.4	15.9
X53250	Zfa	Zinc finger protein, autosomal	15.9	251.1	15.8
D86603	Bach1	BTB and CNC homology 1	15.8	220.4	13.9
D26532	Runx1	Runt related transcription factor 1	62.9	788	12.5
AF084480	Baz1b	Bromodomain adjacent to zinc finger domain, 1B	20.2	242.8	12.0
AF000294	Pparbp	Peroxisome proliferator activated receptor binding protein	40.7	399.8	9.8
AA867655	Pb1-pending	Polybromo 1/2610016F04Rik: RIKEN cDNA 2610016F04 gene	81.1	529.2	6.5
U09504	Nr1d2	Nuclear receptor subfamily 1, group D, member 2	67.6	429	6.3
AF041822	Tbx15	T-box 15	37	232.7	6.3
AF064088	Tieg1	TGF-β-inducible early growth response 1	148.5	895.7	6.0
X60136	Sp1	*trans*-Acting transcription factor 1	80.4	481.1	6.0
Y07836	Bhlhb2	Basic helix–loop–helix domain containing, class B2	434.9	2503.2	5.8
M64068	Bmi1	B lymphoma Mo-MLV insertion region 1	280	1558.2	5.6
AB024005	Zfp68	Zinc finger protein 68	52.8	285.9	5.4
M63725	Atf1	Activating transcription factor 1	171.6	925.5	5.4
D50416	Six4	Sine oculis-related homeobox 4 homolog (Drosophila)	79.3	415.8	5.2
AF010600	Smarca3	SWI/SNF related, matrix associated, actin-dependent regulator of chromatin, subfamily a, member 3	58.5	304.3	5.2
U21855	Cnot7	CCR4-NOT transcription complex, subunit 7	45	231.5	5.1
D76432	Zfhx1a	Zinc finger homeobox 1a	205.5	1052.2	5.1
Cell cycle control					
AF002823	Bub1	Budding uninhibited by benzimidazoles 1 homolog (*S. cerevisiae*)	12.4	235.9	19.0
AF076845	Hus1	Hus1 homolog (*S. pombe*)	22.7	369.2	16.3
AV138783	Gadd45b	Growth arrest and DNA-damage-inducible 45 beta	62.7	779.3	12.4
Z75332	Stag1	Stromal antigen 1	56.4	391.1	6.9
AI846890	Stag2	Stromal antigen 2	60.4	357.4	5.9
AA032310	Smc4l1	SMC4 structural maintenance of chromosomes 4-like 1 (yeast)	84.2	435.5	5.2
Cell adhesion, extracellular matrix component or modiffer					
AF100777	Wisp1	WNT1-inducible signaling pathway protein 1	72.3	1080.2	14.9
U14135	Itgav	Integrin alpha V	27.2	249.1	9.2
Y13185	Mmp10	Matrix metalloproteinase 10	44.2	364.6	8.2
AF009366	Nedd9	Neural precursor cell expressed, developmentally down-regulated gene 9	143.1	1037	7.2
AF014941	Ctsw	Cathepsin W	84.3	587.7	7.0
U41765	Adam9	A disintegrin and metalloproteinase domain 9 (meltrin gamma)	57	397.3	7.0
AF011379	Adam10	A disintegrin and metalloprotease domain 10	150.9	1041.7	6.9
L18880	Vcl	Vinculin	108.9	633.5	5.8
X66473	Mmp13	Matrix metalloproteinase 13	96.8	558.7	5.8
X62622	Timp2	Tissue inhibitor of metalloproteinase 2	637	3644.5	5.7
M82831	Mmp12	Matrix metalloproteinase 12	59.5	323.5	5.4

[a] T, 10 nM testosterone.
[b] +TGF-β, 10 nM testosterone plus 10 ng/ml of recombinant human TGF-β1.

lated from SC-3 cells [12], was also subcloned into a pGL-3 luciferase vector. The constructed plasmids, pGL-3-hPSCA-luc, pGL-3-hPSA-luc and pGL-3-m*fgf8*-luc, together with the pSV2neo Helper Plasmid (CLONTECH Laboratories, Palo Alto, CA, USA) were transfected into SC-3 cells using a lipofectamine reagent (Invitrogen). The cells were selected in the presence of 400 μg/ml G418 (Invitrogen). After allowing 3 weeks for the selection, the stably expressing SC-3 cells were assayed for the luciferase activity as described previously [12]. The data were standardized per microgram protein as measured by a BCA Protein Assay Kit (Pierce, Rockford, IL, USA).

2. Results

2.1. Oligonucleotide microarray analysis

Compared with the data of the testosterone-stimulated SC-3 cells, 165 genes were up-regulated at more than 5-fold, and 78 genes were down-regulated to less than one-third. The top 40 genes are shown in Tables 1 and 2. High-ranking genes are also categorized by their function or cellular localization in Tables 3 and 4. Functional annotations were provided by Mouse Genome Informatics (http://www.informatics.jax.org/).

Of note, *fgf8* was by far the most responsive gene under the TGF-β1 treatment. Other androgen-regulated genes, such as lipocalin 7 [13], apolipopretein D [14] and PSCA [15], were also repressed by TGF-β1 in this analysis (Table 2 and Supplementary data 2). Along with the TGF-β-mediated growth inhibition of the androgen-stimulated SC-3 cells, $p15^{INK4B}$ was induced by TGF-β1 at up to 3.18-fold, while other *CDKI* genes were constantly or marginally expressed in SC-3 cells (Table 5). In addition, the mouse homologue of Myc-interacting zinc finger protein (Miz)-1, Zfp100, was found to be repressed in this analysis (Table 2), possibly correlating with the $p15^{INK4B}$ induction, as previously reported [16]. As reported in a recent paper [17], the repressions of Id1 and 3 were possibly coupled with TGF-β-mediated

Table 4
Summary of down-regulated genes by TGF-β in androgen-stimulated SC-3 cells

Genbank accession	Gene symbol	Description	Microarray data		
			T[a]	+TGF-β[b]	Ratio
Signal transduction molecule					
U74079	Slc9a3r1	Solute carrier family 9 (sodium/hydrogen exchanger), isoform 3 regulator 1	2648	881.6	0.33
AB004879	Mras	Muscle and microspikes RAS	1026	333.6	0.33
AB021861	Map3k6	Mitogen-activated protein kinase kinase kinase 6	920.1	256	0.28
U20238	Rasa3	RAS p21 protein activator 3	834.2	218.9	0.26
U88325	Socs1	Suppressor of cytokine signaling 1	1379	342.6	0.25
AF064984	Lrp5	Low density lipoprotein receptor-related protein 5	657	154.9	0.24
Y17709	Fzd9	Frizzled homolog 9 (Drosophila)	286.6	65.7	0.23
U07634	Epha2	Eph receptor A2	948.2	147.9	0.16
AF044030	Ltb4r1	Leukotriene B4 receptor 1	343.1	46.3	0.13
Cytokine, growth factor or growth factor ligand					
AJ011967	Gdf15	Growth differentiation factor 15	2523	836.2	0.33
D12483	Fgf8	Fibroblast growth factor 8	1620	20.5	0.01
Transcriptional factor or modulator					
D90085	Zfp144	Zinc finger protein 144	206.4	53.3	0.26
X15784	Myog	Myogenin	264.3	66.6	0.25
U14556	Zfp100	Zinc finger protein 100	319.9	79.4	0.25
AW047343	Dbp	D site albumin promoter binding protein	335.8	83.3	0.25
X61800	Cebpd	CCAAT/enhancer binding protein (C/EBP), delta	7501	1815.6	0.24
AW048233	Erf	Ets2 repressor factor	2153	476	0.22
U51743	Tead4	TEA domain family member 4	1169	252	0.22
AF017128	Fosl1	fos-like antigen 1	5166	724.9	0.14
Cell cycle control					
M31885	Idb1	Inhibitor of DNA binding 1	1301	342.1	0.26
M60523	Idb3	Inhibitor of DNA binding 3	621.5	138.8	0.22
Cell adhesion, extracellular matrix component or modiffer					
AF050666	Gpld1	Glycosylphosphatidylinositol specific phospholipase D1	338.6	103.6	0.31
AW209486	Psca	Prostate stem cell antigen	505.3	114	0.23
X78545	Mcpt8	Mast cell protease 8	356.1	78.8	0.22
AF045887	Agt	Angiotensinogen	1201	123	0.10

[a] T, 10 nM testosterone.
[b] +TGF-β, 10 nM testosterone plus 10 ng/ml of recombinant human TGF-β1.

Table 5
Expression profiles of *CDKI* genes in SC-3 cells

Gene name	Microarray data		
	T[a]	+TGF-β[b]	Ratio
Cyclin-dependent kinase inhibitor 2B (p15)	199.3	633.3	3.18
Cyclin-dependent kinase inhibitor 1B (p27)	43	85.1	1.98
Cyclin-dependent kinase inhibitor 2A (p16)	99.8	153.1	1.53
Cyclin-dependent kinase inhibitor 1C (p57)	20.5	25.2	1.23
Cyclin-dependent kinase inhibitor 2C (p18)	597.8	619.6	1.04
Cyclin-dependent kinase inhibitor 1A (p21)	1504.2	1211.2	0.81
Cyclin-dependent kinase inhibitor 2D (p19)	591.4	301	0.51

[a] T, 10 nM testosterone.
[b] +TGF-β, 10 nM testosterone plus 10 ng/ml of recombinant human TGF-β1.

growth arrest. Other growth-suppressive and apoptotic genes, including growth arrest and DNA-damage-inducible 45 β (GADD45β), TGF-β-inducible early growth response 1 (Tieg1), Fas and caspase 3, were also found in the TGF-β-inducible genes (Table 1 and Supplementary data 1). A well-known TGF-β-responsive gene of plasminogen activator inhibitor (PAI)-1 was also induced at 4.67-fold (data not shown), confirming the TGF-β signaling in SC-3 cells.

A considerable number of cell-matrix remodeling genes, including matrix metalloproteinase (MMP) 10, 12 and 13, disintegrin and metalloproteinase domain (Adam) 9 and 10, and a tissue inhibitor of metalloproteinase (TIMP) 2, were also induced by TGF-β1 in this analysis (Tables 1 and 3 and Supplementary data 1). TGF-β also induced several muscle proteins, such as sarcolemma associated protein (Slmap), utrophin and tropomyosin 4, suggesting the differentiation into mesenchymal or myoepithelial phenotypes in SC-3 cells (Tables 1 and 3 and Supplementary data 1). Other TGF-β-responsive molecules reported in previous microarray data [4,17,18], including Runt-related transcription factor (Runx) 1, vascular endothelial growth factor (VEGF) and IQ motif containing GTPase activating protein (IQGAP) 1, were also found in the TGF-β-inducible genes (Tables 1 and 3 and Supplementary data 1). The up-regulation of WNT1-inducible signaling pathway protein (Wisp)-1 and *Wnt* 7B suggests the activation of Wnt-signaling in response to TGF-β (Tables 1 and 3).

The transcriptional level of the androgen receptor gene was unchanged under the TGF-β treatment in SC-3 cells (data not shown).

2.2. Real-time PCR

Given that FGF8 is a critical factor in the androgen-stimulated growth of SC-3 cells, we further examined the

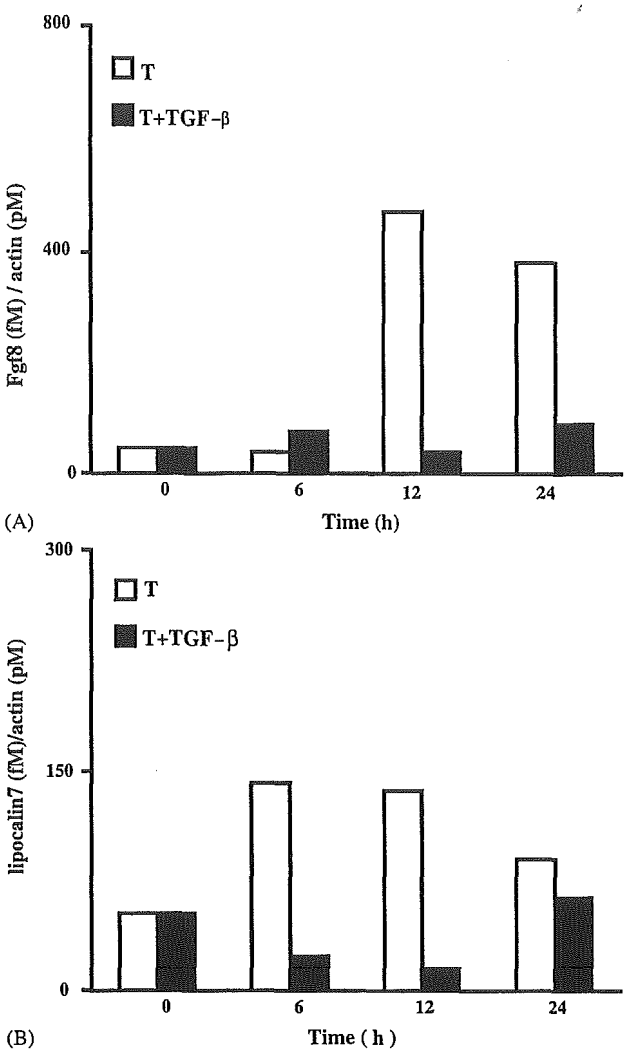

Fig. 1. Real-time PCR analysis on *fgf8* and lipocalin 7 transcripts in testosterone-stimulated SC-3 cells in the absence or presence of TGF-β. SC-3 cells were plated in an androgen-free basal medium, and then stimulated with 10 nM testosterone in the absence (T) or presence of 10 ng/ml TGF-β1 (+TGF-β) under the serum-free condition. RNAs were prepared from SC-3 cells at indicated hours, and the transcriptional levels of *fgf8* (A) and lipocalin 7 (B) were quantitatively analyzed by real-time PCR as described in Section 1.5. The absolute values of the transcripts (fM) were standardized with those of the β-actin transcripts (pM). The results are expressed as the mean of duplicate determinates.

levels of *fgf8* transcripts in the absence or presence of TGF-β1 by real-time PCR. The transcriptional level of *fgf8* in the testosterone-stimulated SC-3 cells reached a 10-fold-induction at 12 h, while its level was severely suppressed in the presence of TGF-β1 (Fig. 1A). Similarly, the transcriptional level of another androgen-regulated gene of lipocalin 7 was also attenuated by TGF-β (Fig. 1B).

2.3. Apoptosis and cell growth analyses

The up-regulation of several apoptotic genes prompted us to investigate the involvement of the apoptotic process in the TGF-β-mediated growth inhibition of SC-3 cells.

The caspase 3 activity remained at marginal levels in the presence of TGF-β1 at 6 and 24 h in SC-3 cells, while TNF-α significantly activated caspase 3 at 6 h (Fig. 2A). In the TUNEL assay, the number of labeled cells was also marginal under the TGF-β1 stimulation at 6 and 24 h, contrasted with the data of the TNF-α treatment in SC-3 cells (Fig. 2B and C). In addition, the treatment with TGF-β1 on androgen-stimulated SC-3 cells showed relative G1-arrest in contrast with the androgen-stimulated control in a flow cytometer (Fig. 2D). All these findings clearly indicate the cell-static effect of TGF-β on the androgen-stimulated SC-3 cells.

Next, we investigated the effect of TGF-β on FGF8-simulated growth in SC-3 cells. The MTT assay clearly demonstrated that TGF-β fails to suppress the FGF8-stimulated growth of SC-3 cells (Fig. 2E). Additional experiment using stably FGF8-expressing SC-3 cells also gave us similar results (Fig. 2F). Both findings strongly

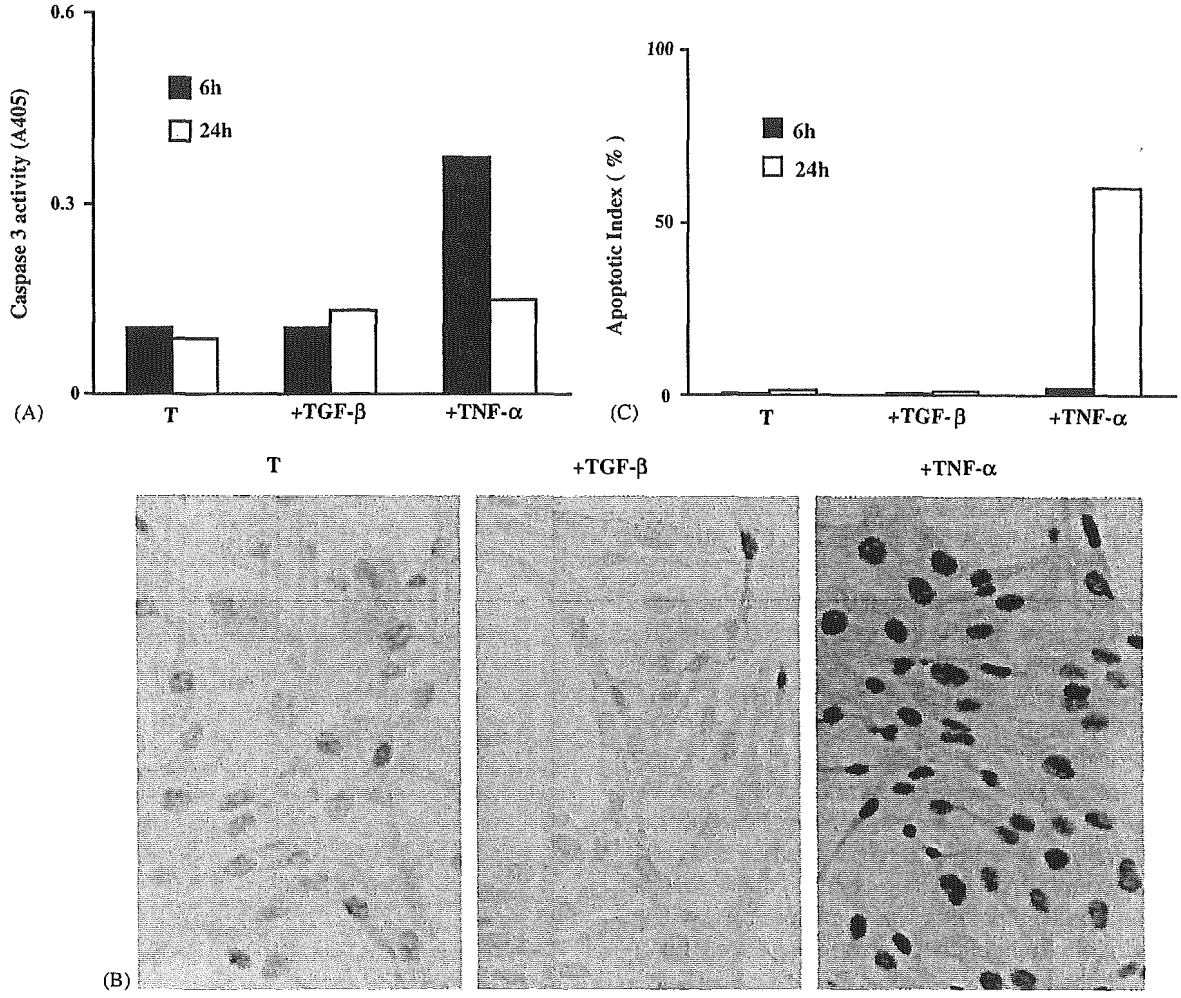

Fig. 2. Apoptosis and cell growth analyses under the TGF-β treatment in SC-3 cells. Effects of TGF-β on the caspase 3 activity in androgen-stimulated SC-3 cells (A). SC-3 cells were plated, and stimulated with 10 nM testosterone in the absence (T) or presence of 10 ng/ml TGF-β1 (+TGF-β). After the indicated hours, the cell lysates were collected, and assayed for caspase 3 activity using the Ac-DEVD-pNA substrate. Analysis of apoptotic processes in response to TGF-β by the TUNEL method (B and C). SC-3 cells were plated, and stimulated with 10 nM testosterone in 4-well-chamber slides in the absence (T) or presence of 10 ng/ml TGF-β1 (+TGF-β). The slides were fixed with 1% paraformaldehyde after the indicated hours of incubation. Cells incorporating digoxigenin-conjugated dNTP at the nucleotide nick ends were detected by peroxidase-based immunocytochemistry. The slides were photographed, and the ratios of positive cells in four different areas were counted. Immunostainings at 24 h are shown in (B). The ratios are expressed as the mean ± S.E.M. (C). In both studies, 5 ng/ml of TNF-α (+TNF-α) was used as the positive control. Flow cytometric analysis (D). SC-3 cells were plated in a protein-free basal medium in the absence of androgen. After incubation for 24 h, the cells were treated or untreated (—) with 10 nM testosterone (T) in the presence or absence of 10 ng/ml TGF-β1 (+ TGF-β). After incubation for 24 h, the cells were collected and fixed with 1% paraformaldehyde. The cells at 0 h were also collected (0 h). After being stained with propiodium iodide, DNA contents were analyzed by a flow cytemeter. Percents of G1 phase were 79.16%; at 0 h, 78.90%; in untreated cells, 33.32%; in testosterone-stimulated cells, 51.55%; in cells treated testosterone plus TGF-β, respectively. Effects of TGF-β on the FGF8-simulated growth of SC-3 cells (E and F). SC-3 cells were plated in an androgen-free basal medium, and then stimulated with 50 ng/ml FGF8 in the presence or absence of various concentrations of TGF-β1 under a serum-free condition (E). Similarly, stably FGF8-expressing SC-3 cells were plated and cultured in the absence or presence of various concentrations of TGF-β1 (F). Cell growth was measured by the MTT method after 72 h of incubation. The results are expressed as the mean ± S.E.M. of triplicate determinants. The other trial showed similar results.

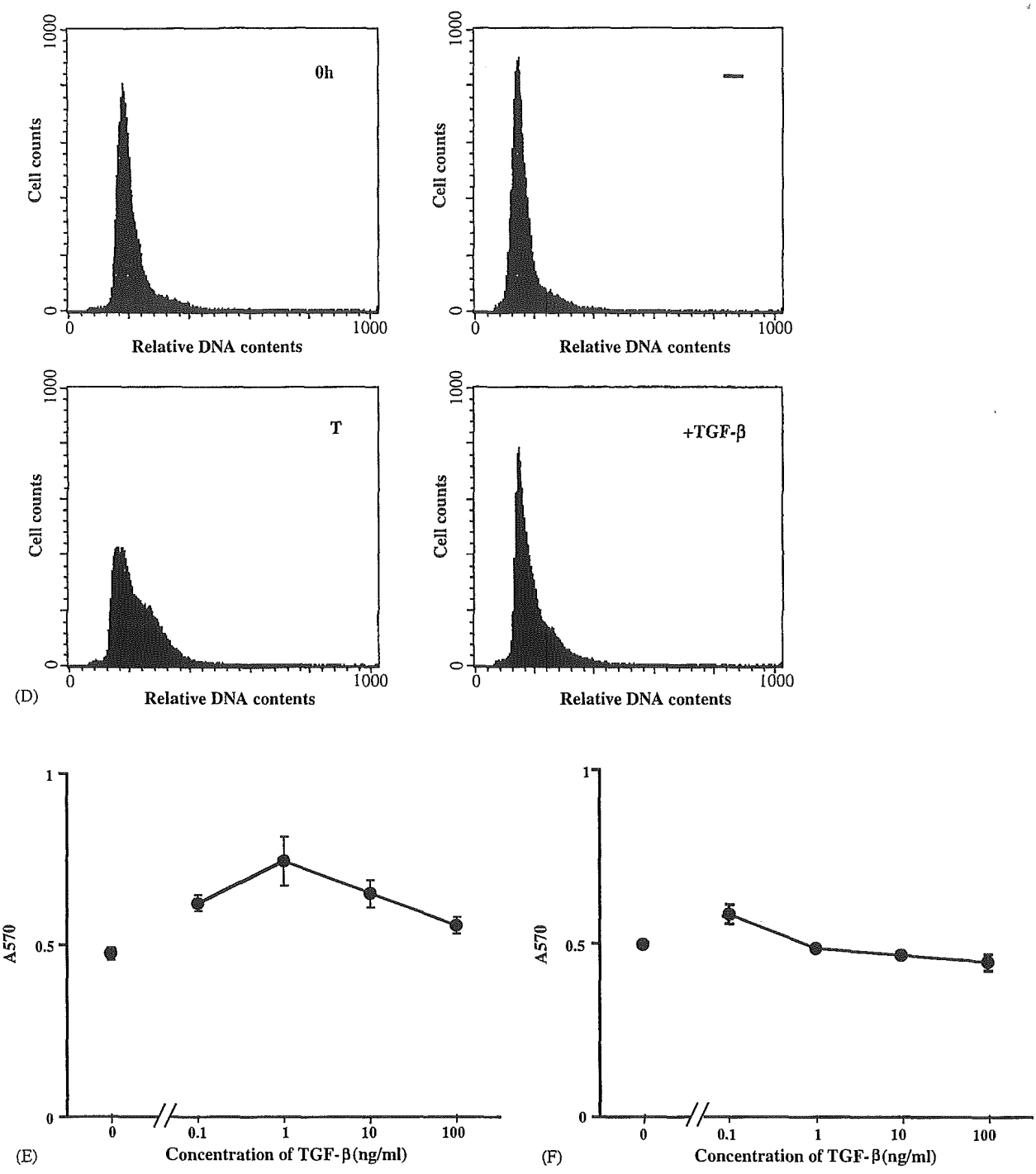

Fig. 2. (*Continued*).

suggest that the transcriptional repression of *fgf8* is required for the TGF-β-mediated growth arrest in SC-3 cells.

2.4. Attenuation of the androgen-responsive promoter activity by TGF-β in SC-3 cells

Next, we investigated the effect of TGF-β on a couple of androgen-responsive promoters. Because the androgen-regulated region in the *fgf8* locus still remains undefined, we used the well-known androgen-responsive promoters of PSA and PSCA in this study. In stably transfected SC-3 cells either with pGL-3-hPSA-luc or pGL-3-hPSCA-luc, the treatment with TGF-β1 significantly suppressed the androgen-responsive reporter activity (Fig. 3A and B). On the other hand, the androgen-unresponsive core promoter activity of the *fgf8* gene was unchanged in the presence of TGF-β (Fig. 3C).

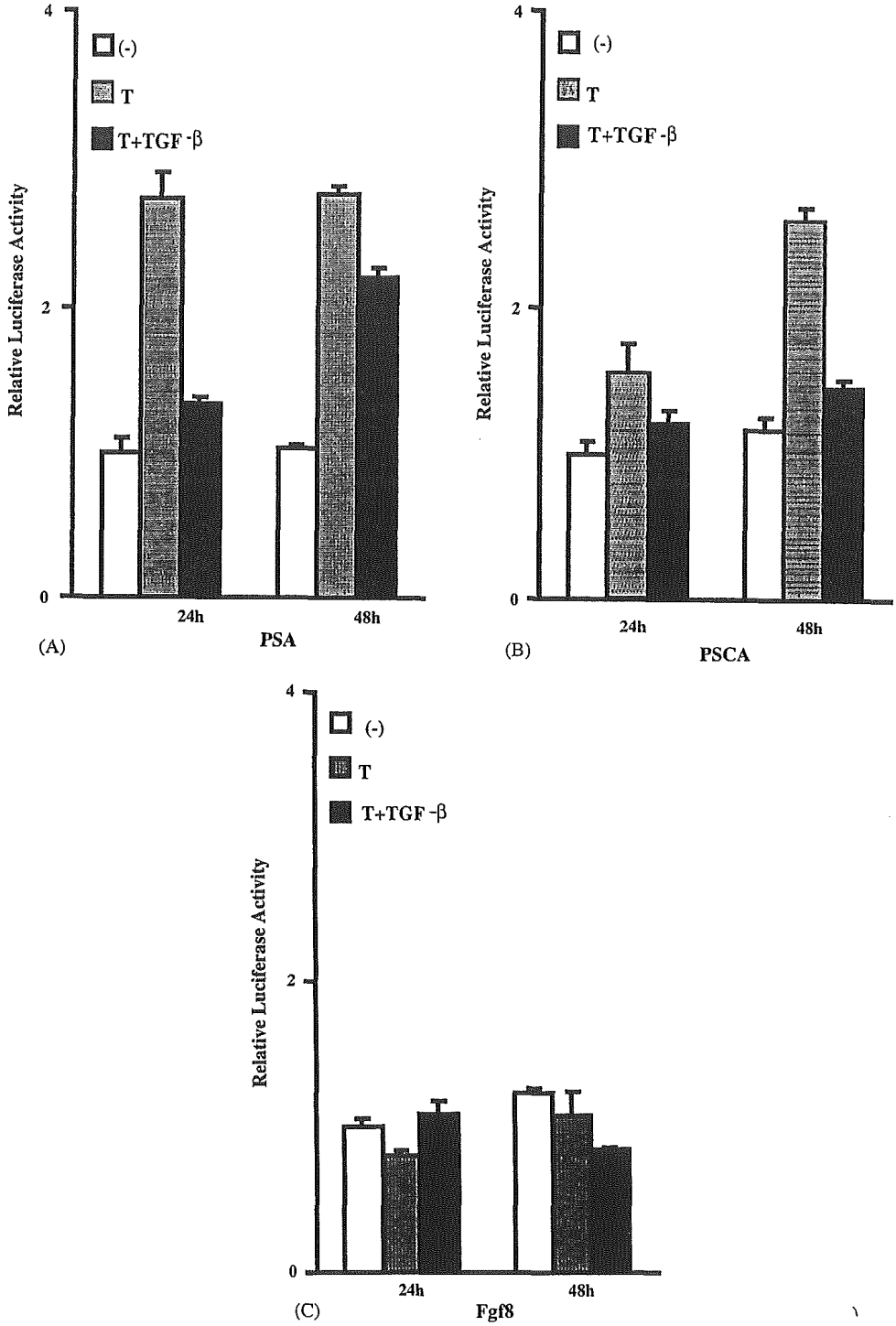

Fig. 3. Effects of TGF-β on the androgen-regulated reporters or the androgen-unresponsive core promoter of the *fgf8* gene in SC-3 cells. SC-3 cells stably transfected with pGL-3-hPSA-luc (A), pGL-3-hPSCA-luc (B), or pGL-3-m*fgf8*-luc (C) were plated and cultured in an unstimulated condition (—), or stimulated with 10 nM testosterone in the absence (T) or presence of TGF-β1 (+TGF-β). After 24 and 48 h of incubation, the cell extracts were collected and assayed for the luciferase activity. Values of luciferase activity were shown as fold ratios with each unstimulated sample at 24 h after standardization with protein concentrations. The results are expressed as the mean ± S.E.M. of triplicate determinants.

3. Discussion

The present microarray analysis clearly demonstrated that *fgf8* was by far the most markedly regulated gene in response to TGF-β in SC-3 cells. The present real-time PCR confirmed the transcriptional repression of *fgf8* by TGF-β. Importantly, *fgf8* is well known as an essential growth factor in the androgen-dependent growth of SC-3 cells. Therefore,

it is highly likely that the repression of *fgf8* is tightly coupled with the TGF-β-mediated growth inhibition in SC-3 cells. Earlier reports have shown that CDKIs and the caspase family are involved in TGF-β-mediated growth inhibition [19,20]. In fact, one of the CDKIs, $p15^{INK4B}$, was induced by TGF-β in SC-3 cells. In addition, apoptotic effector genes of Fas and caspase 3 were also up-regulated by TGF-β in SC-3 cells. Nevertheless, the up-regulation of these molecules was insufficient to lead SC-3 cells to apoptosis within 24 h, as judged by both the TUNEL method and the caspase 3 activity assay. In addition, treatment with TGF-β failed to suppress the cell growth stimulated by exogenous FGF8 in SC-3 cells, suggesting that the transcriptional repression of *fgf8* is required for the TGF-β-mediated growth inhibition. It is very important to elucidate the mechanisms involved in the transcriptional repression of *fgf8* by TGF-β because both growth factors play critical roles on embryogenesis and tumorigenesis. However, our lack of knowledge about the regulatory mechanism of the *fgf8* gene expression by androgens prevents us from taking a direct approach on this issue. Given that the core promoter activity of the *fgf8* gene was not affected by TGF-β in SC-3 cells, it is less possible that a general transcriptional repressor is involved in the repression of *fgf8*. It is rather possible that TGF-β might interrupt the transcriptional cascades induced by androgens, leading to the transcriptional repression of *fgf8*. In support of this notion, the androgen-responsive reporter activity is actually attenuated by TGF-β in SC-3 cells. In fact, a couple of androgen-responsive genes are down-regulated by TGF-β. Based on these findings, it is most likely that some of the androgen-inducible genes are physiological targets of the TGF-β-mediated signaling, and this led us to speculate that the repression of *fgf8* might be directly or indirectly involved in this process.

In recent studies, TGF-β has also been shown to facilitate aggressive and invasive phenotypes in carcinomas through the EMT process [21,22]. The induction of a considerable number of cell-matrix remodeling genes and mesenchymal genes by TGF-β suggests that TGF-β also promotes an EMT phenotype in SC-3 cells. In this sense, SC-3 cells that have escaped from TGF-β-mediated growth arrest might show more aggressive phenotypes through EMT. The cellular balance between the growth-inhibitory effect and the more aggressive phenotype of EMT induced by TGF-β is a next important issue to be explored.

Acknowledgments

We would like to thank Dr. K. Shitara at the Tokyo Research Laboratories of Kyowa Hakko Kogyo for his kind gift of FGF8-expressing plasmid. We also would like to thank Dr. Y. Furukawa at Jichi Medical School and Dr. J. Ohuchi at the Pharmaceutical Research Institute of Kyowa Hakko Kogyo for their helpful advice.

Appendix A. Supplementary data

Supplementary data associated with this article can be found, in the online version, at doi:10.1016/j.jsbmb.2005.01.031.

References

[1] R. Derynck, Y.E. Zhang, Smad-dependent and Smad-independent pathways in TGF-β family signalling, Nature 425 (6958) (2003) 577–584.
[2] M.G. Alexandrow, H.L. Moses, Transforming growth factor β and cell cycle regulation, Cancer Res. 55 (7) (1995) 1452–1457.
[3] J. Massagué, S.W. Blain, R.S. Lo, TGFβ signaling in growth control, cancer, and heritable disorders, Cell 103 (2) (2000) 295–309.
[4] J. Zavadil, M. Bitzer, D. Liang, Y.C. Yang, A. Massimi, S. Kneitz, E. Piek, E.P. Böttinger, Genetic programs of epithelial cell plasticity directed by transforming growth factor-β, Proc. Natl. Acad. Sci. U.S.A. 98 (12) (2001) 6686–6691.
[5] F. Verrecchia, M.L. Chu, A. Mauviel, Identification of novel TGF-β/Smad gene targets in dermal fibroblasts using a combined cDNA microarray/promoter transactivation approach, J. Biol. Chem. 276 (20) (2001) 17058–17062.
[6] S.A. Hayes, M. Zarnegar, M. Sharma, F. Yang, D.M. Peehl, P. ten Dijke, Z. Sun, SMAD3 represses androgen receptor-mediated transcription, Cancer Res. 61 (5) (2001) 2112–2118.
[7] A. Tanaka, K. Miyamoto, N. Minamino, M. Takeda, B. Sato, H. Matsuo, K. Matsumoto, Cloning and characterization of an androgen-induced growth factor essential for the androgen-dependent growth of mouse mammary carcinoma cells, Proc. Natl. Acad. Sci. U.S.A. 89 (19) (1992) 8928–8932.
[8] A. Tanaka, K. Miyamoto, H. Matsuo, K. Matsumoto, H. Yoshida, Human androgen-induced growth factor in prostate and breast cancer cells: its molecular cloning and growth properties, FEBS Lett. 363 (3) (1995) 226–230.
[9] A. Tanaka, A. Furuya, M. Yamasaki, N. Hanai, K. Kuriki, T. Kamiakito, Y. Kobayashi, H. Yoshida, M. Koike, M. Fukayama, High frequency of fibroblast growth factor (FGF) 8 expression in clinical prostate cancers and breast tissues, immunohistochemically demonstrated by a newly established neutralizing monoclonal antibody against FGF 8, Cancer Res. 58 (10) (1998) 2053–2056.
[10] A. Tanaka, T. Kamiakito, N. Takayashiki, S. Sakurai, K. Saito, Fibroblast growth factor 8 expression in breast carcinoma: associations with androgen receptor and prostate-specific antigen expressions, Virchow Arch. 441 (4) (2002) 380–384.
[11] H. Yamanishi, N. Nonomura, A. Tanaka, T. Yasui, Y. Nishizawa, K. Matsumoto, B. Sato, Roles of transforming growth factor β in inhibition of androgen-induced growth of Shionogi carcinoma cells in serum-free medium, Cancer Res. 50 (19) (1990) 6179–6183.
[12] K. Kuriki, T. Kamiakito, H. Yoshida, K. Saito, M. Fukayama, A. Tanaka, Integration of proviral sequences, but not at the common integration sites of the FGF8 locus, in an androgen-dependent mouse mammary Shionogi carcinoma, Cell. Mol. Biol. 46 (7) (2000) 1147–1156.
[13] M. Kobayashi, T. Kinouchi, Y. Hakamata, T. Kamiakito, K. Kuriki, K. Suzuki, A. Tokue, M. Fukayama, A. Tanaka, Isolation of an androgen-inducible novel lipocalin gene, Arg1, from androgen-dependent mouse mammary Shionogi carcinoma cells, J. Steroid Biochem. Mol. Biol. 77 (2–3) (2001) 109–115.
[14] J. Simard, Y. de Launoit, D.E. Haagensen, F. Labrie, Additive stimulatory action of glucocorticoids and androgens on basal and estrogen-repressed apolipoprotein-D messenger, ribonucleic acid levels and secretion in human breast cancer cells, Endocrinology 130 (3) (1992) 1115–1121.

[15] A. Jain, A. Lam, I. Vivanco, M.F. Carey, R.E. Reiter, Identification of an androgen-dependent enhancer within the prostate stem cell antigen gene, Mol. Endocrinol. 16 (10) (2002) 2323–2337.
[16] K. Peukert, P. Staller, A. Schneider, G. Carmichael, F. Hänel, M. Eilers, An alternative pathway for gene regulation by Myc, EMBO J. 16 (18) (1997) 5672–5686.
[17] Y. Kang, C.R. Chen, J. Massague, A self-enabling TGFβ response coupled to stress signaling: Smad engages stress response factor ATF3 for Id1 repression in epithelial cells, Mol. Cell. 11 (4) (2003) 915–926.
[18] L. Xie, B.K. Law, M.E. Aakre, M. Edgerton, Y. Shyr, N.A. Bhowmick, H.L. Moses, Transforming growth factor beta-regulated gene expression in a mouse mammary gland epithelial cell line, Breast Cancer Res. 5 (6) (2003) 187–198.
[19] G.J. Hannon, D. Beach, p15INK4B is a potential effector of TGF-β-induced cell cycle arrest, Nature 371 (6494) (1994) 257–261.
[20] R.H. Chen, T.Y. Chang, Involvement of caspase family proteases in transforming growth factor-β-induced apoptosis, Cell Growth Differ. 8 (7) (1997) 821–827.
[21] W. Cui, D.J. Fowlis, S. Bryson, E. Duffie, H. Ireland, A. Balmain, R.J. Akhurst, TGFβ1 inhibits the formation of benign skin tumors, but enhances progression to invasive spindle carcinomas in transgenic mice, Cell 86 (4) (1996) 531–542.
[22] M. Oft, K.H. Heider, H. Beug, TGFβ signaling is necessary for carcinoma cell invasiveness and metastasis, Curr. Biol. 8 (23) (1998) 1243–1252.

Pathology International 2005; **55**: 63–69

Original Article

Distinct expression patterns of claudin-1 and claudin-4 in intraductal papillary–mucinous tumors of the pancreas

Munetoshi Tsukahara,[1] Hideo Nagai,[1] Tomoko Kamiakito,[2] Hirotoshi Kawata,[2] Norio Takayashiki,[2] Ken Saito[2] and Akira Tanaka[2]

Departments of [1]Surgery and [2]Pathology, Jichi Medical School, Minamikawachi, Kawachi, Tochigi, Japan

The expression of claudin-4 was investigated in human pancreas, pancreatic ductal adenocarcinomas, and intraductal papillary–mucinous tumors of the pancreas (IPMT), and compared with that of claudin-1. In human adult pancreatic specimens, both claudin-1 and claudin-4 were immunohistochemically found in main and branching pancreatic ducts, terminal ductules and acinic cells, with the exception of endocrine cells. Of 12 cases of pancreatic ductal adenocarcinoma, 11 (92%) had positive immunostaining for claudin-4, and seven (58%) for claudin-1. In 44 lesions of 22 cases of IPMT, including six hyperplastic foci distant from the main lesions, clauidin-1 was positive in three out of six (50%) hyperplastic foci, 14 out of 17 (82%) adenomas, three out of 10 (30%) borderline tumors, two out of six (33%) non-invasive carcinomas, and one out of five (20%) invasive carcinomas, producing a statistically negative correlation with histological tumor grades. In contrast, claudin-4 was negative in the six hyperplastic foci, and positive in four out of the 17 (24%) adenomas, five out of the 10 (50%) borderline tumors, five out of the six (83%) non-invasive carcinomas, and four out of the five (80%) invasive carcinomas, producing a statistically positive correlation with histological tumor grades. On study of IPMT subtypes, claudin-1 was positive in nine out of 10 (90%) clear-cell types, seven out of 20 (35%) dark-cell types, and four out of eight (50%) compact-cell types. In contrast, claudin-4 was positive in two out of the 10 (20%) clear-cell types, 13 out of the 20 (65%) dark-cell types, and three out of the eight (38%) compact-cell types. These distinct expression patterns of claudin-1 and claudin-4 suggest that both claudins serve as useful molecular markers for the tumor classification of IPMT.

Correspondence: Akira Tanaka, MD, PhD, Department of Pathology, Jichi Medical School, 3311-1 Yakushiji, Minamikawachi, Kawachi, Tochigi 329-0498, Japan. Email: atanaka@jichi.ac.jp

Received 16 June 2004. Accepted for publication 31 October 2004.

Key words: claudin-1, claudin-4, intraductal papillary-mucinous tumor of the pancreas, pancreas

A tight junction is an intercellular adhesion structure forming a permeability barrier at apical portions, as well as giving cellular polarity to epithelial cells.[1,2] Claudins are essential components of the tight junction, consisting of at least 20 proteins.[3] Given that cellular polarity is frequently distorted in cancers, it is speculated that claudins are dysregulated in various cancers. The overexpression of claudin-3 or claudin-4 has been shown in pancreatic, ovarian, and prostatic cancers.[4–6] In particular, claudin-4 has been reported as playing an important role in the growth, invasion, and metastasis of pancreatic cancers.[7] Pancreatic ductal adenocarcinomas are the most common tumor types in the pancreas, but are also well known for having a very poor prognosis. In contrast, intraductal papillary–mucinous tumors (IPMT) are a distinct entity of pancreatic exocrine tumors.[8] In general, IPMT are subclassified into adenomas, borderline tumors, and carcinomas on the basis of their cellular and structural atypia, and are thought to be subject to an adenoma–carcinoma sequence.[9] In addition, non-invasive IPMT carcinomas have favorable prognoses, compared with pancreatic ductal adenocarcinomas.[9] These characteristics of IPMT prompted us to investigate the correlation between claudin-4 expression and the tumor grades of IPMT. In the present study we used claudin-1 as a comparison. Claudin-1 is the first member of claudins involved in the epidermal barrier formation with claudin-4.[10,11] A recent report has demonstrated the frequent upregulation of claudin-1 in colorectal cancers, suggesting its involvement in gastrointestinal tumorigenesis.[12] In the present study we analyzed claudin-1 and claudin-4 expression in human pancreatic tissues, pancreatic ductal adenocarcinomas, and IPMT using immunohistochemistry and real-time polymerase chain reaction (PCR).

MATERIALS AND METHODS

Samples

Formalin-fixed and paraffin-embedded sections of human pancreas, pancreatic ductal adenocarcinomas, and IPMT were retrieved from the files at Jichi Medical School. The patient profiles of the 22 cases of IPMT are summarized in Table 1. The histological tumor grades were re-evaluated by the three authors (MT, KS and AT). In general, neoplastic lesions without atypia were classified as adenomas, and intraepithelial neoplastic lesions with marked atypia, mostly adjacent to invasive carcinomas, were classified as carcinoma *in situ*. Atypical lesions between the adenoma and carcinoma *in situ* were grouped as borderline tumors. Every histological grade in the 22 cases (38 lesions in total) was investigated. In addition, six hyperplastic foci distant from the main lesions were also investigated. IPMT are also subgrouped into a dark-cell type (nine cases), a clear-cell type (nine cases), and a compact-cell type (four cases) using MUC2 and MUC5AC immunostainings as previously reported.[13] Twelve patients with pancreatic ductal adenocarcinomas (eight with moderately differentiated and four with well-differentiated types) had ages ranging from 53 to 77 years (median, 69.5 years) and a gender ratio of 5:7 (female : male). Three patients with mild pancreatitis, one case from an islet cell tumor, and four cases from carcinomas of the Vater's ampulla or common bile duct were used as normal controls, with ages ranging from 34 to 78 years (median: 55 years), and a gender ratio of 6:2 (female : male). In addition, cDNA specimens (two of ductal carcinomas, four of IPMT, and three of normal pancreatic tissues distant from the main lesion of pancreatic tumors), previously prepared at Jichi Medical School, were used for real-time PCR under the approval of the local ethics committee at Jichi Medical School.

Immunohistochemistry

The monoclonal antibody against human claudin-4, and the polyclonal antibody against human claudin-1 were purchased from Zymed Laboratories (South San Francisco, CA, USA). Formalin-fixed, paraffin-embedded sections were boiled in a microwave oven for 15 min. They were then allowed to interact with each antibody (1:100 dilution for the anticlaudin-1 antibody and 1:400 for the anticlaudin-4 antibody) at 4°C overnight, and stained by an avidin–biotin complex method. The immunostaining results were scored as follows according to a previous report conducted by us:[14] –, negative staining; ±, diffuse weak cytoplasmic staining or focal positive membrane staining; +, distinctly positive membrane staining in more than 20–30% of the tumor areas; ++, strongly positive membrane staining in more than 20–30% of the tumor areas. The categories of '+' and '++' were judged as positive.

Cells

Human pancreatic cancer PANC-1 cells were purchased from Dainippon Pharmacy (Osaka, Japan). PANC-1 cells were maintained in a DMEM medium supplemented with 10% fetal bovine serum (FBS).

Table 1 Patient profiles of IPMT of the pancreas

No.	Age (years)	Gender	Location	Tumor grades	Subtypes
1	65	M	Head	Ad (Hy)	Clear
2	70	M	Body	Ad (Hy)	Clear
3	73	F	Body	Ad (Hy)	Clear
4	56	F	Head	Ad	Clear
5	66	M	Head	Ad	Clear
6	73	M	Body	Ad	Clear
7	72	F	Body	Ad	Clear
8	40	M	Head	Ad	Dark
9	55	M	Body	Ad	Clear
10	56	M	Head	Ad	Compact
11	71	F	Head	Ad, B (Hy)	Compact
12	58	M	Body	Ad, B	Clear
13	75	F	Body	Ad, B	Dark
14	66	F	Head	B, Ad (Hy)	Compact
15	75	M	Body	B, Ad	Dark
16	64	M	Head	B	Dark
17	66	M	Head	B, Ca	Dark
18	70	F	Body	B, Ca, Inv. Ca	Compact
19	53	M	Head	B, Ca, Inv. Ca	Dark
20	74	M	Head	Ca, Inv. Ca, Ad	Dark
21	62	F	Body	Ca, Inv. Ca, B, Ad (Hy)	Dark
22	70	M	Head	Ca, Inv. Ca	Dark

Tumor grades: Ad, adenoma; B, borderline lesions; Ca, non-invasive carcinoma; Inv. Ca, invasive carcinoma. The main lesion is represented at the top. Six hyperplastic foci distant from tumors (Hy) were also investigated. IPMT, intraductal papillary–mucinous tumor: clear, clear-cell type; dark, dark-cell type; compact, compact-cell type.